

**A Spatial Analysis of Green Roof Effectiveness for Reducing Urban Heat and Flood Risk in  
the Montreal Region**

By

Ankit Kumar

A Thesis

In the Department

Of

Building Civil and Environmental Engineering

Supervisor

Ursula Eicker

Presented in Partial Fulfillment of the Requirements  
for the Degree of Master of Applied Science (Building Engineering) at

Concordia University

Montréal, Québec, Canada

September 2025

© Ankit Kumar, 2025

**CONCORDIA UNIVERSITY**  
**SCHOOL OF GRADUATE STUDIES**

This is to certify that the thesis prepared

By: **Ankit Kumar**

Entitled: **A Spatial Analysis of Green Roof Effectiveness for Reducing Urban  
Heat and Flood Risk in the Montreal Region**

and submitted in partial fulfillment of the requirements for the degree of

**Master of Applied Science (Building Engineering)**

complies with the regulations of the University and meets the accepted standards with respect to originality and quality.

Signed by the final examining committee:

\_\_\_\_\_ Examiner

Dr. Caroline Hachem-Vermette

\_\_\_\_\_ Examiner

Dr. Pascale Biron

\_\_\_\_\_ Supervisor

Dr. Ursula Eicker

Approved by \_\_\_\_\_

\_\_\_\_\_ Dean of Faculty

## **Abstract**

### **A Spatial Analysis of Green Roof Effectiveness for Reducing Urban Heat and Flood Risk in the Montreal Region**

**Ankit Kumar**

Urbanization exacerbates interconnected environmental challenges, most critically the Urban Heat Island (UHI) effect and increased flood risk. The Montreal region, with its urban island geography, is particularly vulnerable to the cumulative effects of climate change. Therefore, there is a requirement for integrated assessments that can analyze and synthesize the cumulative benefits of nature-based solutions. The current thesis fills this literature gap by quantifying the cumulative effects of large-scale green roof implementation for mitigating UHI and urban flood risk simultaneously.

The methodology integrates two analytical approaches. First, a flood risk map of the Montreal area was generated on a Geographic Information System (GIS) platform, which incorporates the Analytic Hierarchy Process (AHP) procedure, which systematically weigh the following hydrologic factors: drainage density, elevation, stream distances, and precipitation. Second, the ENVI-MET microclimate simulation software was used to calculate the microclimate effect of green roofs on a dense urban study area under normal and extreme heat conditions.

The results state significant climate resilience benefits. The microclimate model conclude that the use of green roofs can contribute to lowering pedestrian level air temperatures by up to 2.16°C on the peak summer day. Furthermore, the hydrological analysis concludes that the installation of green roofs across the whole region could yield significant changes in the levels of flood risk, with over 55% of the region showing decreased levels of flood risk. Therefore, the integration of data on projected microclimate changes and risk analysis provides clear, data-driven information for the urban planners, policymakers that green infrastructure is an essential component in making a city more resilient and sustainable.

## **Acknowledgements**

*Foremost, I would like to express my sincere gratitude to my supervisor Prof. Ursula Eicker, PhD, for the continuous support of my master's study and research, for her patience, motivation, enthusiasm, and immense knowledge. Her guidance helped me all the time in my research and writing of this thesis.*

*Besides my supervisor, I would like to thank all the members from Next-Generation Cities Institute for their encouragement, insightful comments, and valuable feedback. I offer my sincere appreciation for the learning opportunities provided by my lab mates.*

*Last but not least, I would like to express my deepest gratitude to my beloved father Tek Ram Shammi and my mother Mamta Shammi. It would not have been possible for me to become who I am today without your endless support, wise advice, and prayers. I am also extremely grateful to my brother, Atul, and my sister, Shilpi, for their continuous support and unconditional love throughout my life.*

# Table of Contents

<b>Abstract.....</b>	<b>iii</b>
<b>Acknowledgements .....</b>	<b>iv</b>
<b>List of Table.....</b>	<b>viii</b>
<b>List of Figures.....</b>	<b>ix</b>
<b>Chapter 1 Introduction.....</b>	<b>1</b>
1.1 Background .....	1
1.2 Problem Statement .....	2
1.3 Research Questions .....	3
1.4 Thesis Structure .....	3
<b>Chapter 2 Background and Literature Review.....</b>	<b>4</b>
2.1 Urban Heat Island .....	4
2.1.1 What causes Urban heat island effect? .....	6
2.1.2 UHI in urban climatology .....	8
2.1.3 Local Climate Zone Classification.....	8
2.1.4 Advantages of considering Local Climate Zones: .....	9
2.1.5 Mitigation Strategies .....	10
2.1.6 Urban Heat Island classification Montreal .....	12
2.1.7 Link to Green Roofs: .....	13
2.2 Urban Flood Risk Assessment .....	13
2.2.1 Flood Risk Exacerbation by Climate Change .....	14
2.2.2 Role of Urbanization and Land-Use Changes .....	14
2.3 Synergies between Urban Heat and Flood Risks .....	14
2.4 State-of-the-Art: UHI and Flood Mapping .....	15
2.4.1 Global Approaches to Urban Heat Island (UHI) Assessment .....	15
2.4.2 Global Approaches to Urban Flood Risk Assessment .....	15
2.4.3 Identifying the Research Gap.....	16

<b>Chapter 3 Methodology .....</b>	<b>17</b>
3.1 Flood Risk Mapping .....	17
3.1.1 Analytical Framework and Criteria Selection.....	19
3.1.2 Weighting and Consistency Evaluation .....	23
3.1.3 The Analytic Hierarchy Process .....	23
3.1.4 Base Line Flood Risk Map Generation.....	25
3.2 Green Roof Scenario Methodology .....	25
3.2.1 Phase I: Model Parameterization .....	26
3.2.2 Phase II: Creation of New Flood Map and Comparative Analysis.....	26
3.3 Microclimate (UHI) Modelling.....	27
3.3.1 Tool Used in this study - ENVI-MET.....	27
3.3.2 Basic Model and Simulation with ENVI-Met: .....	28
3.3.3 Why is ENVI-Met used for this study?.....	28
3.3.4 Flow Chart .....	29
3.3.5 Data Collection .....	29
3.3.6 Study Area Selection.....	30
3.3.7 Local Climate Zone.....	30
3.3.8 Study Area .....	30
3.3.9 Seasonality in Montreal – Case Study Specifics.....	31
3.3.10 Data Preparation for ENVI-Met.....	32
3.3.11 Simulation Details:.....	32
3.3.12 Weather Data of the Selected Days .....	34
3.3.13 Simulations: .....	34
3.3.14 Study Area Model in Envi-MET.....	35
3.3.15 Simulation File Generation .....	36
<b>Chapter 4 Result and Discussion .....</b>	<b>37</b>
4.1 Effect of Increased Vegetation on Flood Risk Map of the Region .....	37
4.2 Impact of Green Roofs on Urban Heat Island Mitigation.....	38
4.2.1 Simulation Design.....	38
4.2.2 Comparative Analysis .....	39
4.2.3 Impact of Green Roofs on Pedestrian-Level Temperature during a Peak Summer Day .....	43

4.2.4 Comparison of 24-Hour Pedestrian-Level Air Temperature with and without Green Roofs .....	44
4.3 Discussion of Synergistic Benefits .....	45
<b>Chapter 5 Conclusion, Limitations of the Study and Future Works .....</b>	<b>46</b>
5.1 Conclusion .....	46
5.2 Research Questions .....	47
5.3 Limitations of the Study.....	49
5.4 Future Work .....	50
<b>Bibliography .....</b>	<b>52</b>

## List of Table

<i>Table 1. Data Sources for the raw GIS data.....</i>	<i>18</i>
<i>Table 2. Score Index .....</i>	<i>24</i>
<i>Table 3. Layer Weightage.....</i>	<i>25</i>
<i>Table 4. Simulation Detail .....</i>	<i>32</i>
<i>Table 5. Model Parameters.....</i>	<i>32</i>
<i>Table 6. Material Detail .....</i>	<i>33</i>
<i>Table 7. Tree Data .....</i>	<i>33</i>
<i>Table 8. Simulation Scenarios .....</i>	<i>36</i>

## List of Figures

<i>Figure 1. Urban Heat Island</i> .....	4
<i>Figure 2. Historical Average Monthly Temperature (2013-2024)</i> .....	5
<i>Figure 3. Temperature Trend Over the Year 2013-2024</i> .....	5
<i>Figure 4. Processes contributing to urban heat islands at regional and microscales</i> .....	7
<i>Figure 5. Adverse effects of UHI</i> .....	8
<i>Figure 6. Local Climate Zone classification</i> .....	9
<i>Figure 7. Schematic of roofing surfaces subject to incident solar energy</i> .....	11
<i>Figure 8. Types of Green roof system and typical components</i> .....	12
<i>Figure 9. UHI Montreal</i> .....	13
<i>Figure 11: Overall Thesis Structure</i> .....	17
<i>Figure 11: Methodology for Flood Risk Mapping</i> .....	19
<i>Figure 12. Drainage Density Layer</i> .....	20
<i>Figure 13. Annual Precipitation Layer</i> .....	21
<i>Figure 14. Distance to Stream Layer</i> .....	22
<i>Figure 15. Elevation Layer</i> .....	23
<i>Figure 16. Methodology Flow Chart</i> .....	29
<i>Figure 17. Local Climate Zones – Montreal Region</i> .....	30
<i>Figure 18. Study Area</i> .....	31
<i>Figure 19. Weather Data</i> .....	34
<i>Figure 20. Full Study Area Model</i> .....	35
<i>Figure 21. Green Roof Installed</i> .....	36
<i>Figure 22. Conventional Roof</i> .....	36
<i>Figure 23. Original Flood Risk Map</i> .....	37
<i>Figure 24. Modified Flood Risk Map</i> .....	37
<i>Figure 25: Temperature Difference on General Summer Day at Max Temperature</i> .....	39
<i>Figure 26: Temperature Difference on Peak Summer Day at Max Temperature</i> .....	40
<i>Figure 27: Temperature Difference on General Summer Day at Min Temperature</i> .....	41
<i>Figure 28: Temperature Difference on Peak Summer Day at Min Temperature</i> .....	42
<i>Figure 29: Effect of building elevation on pedestrian level temperature</i> .....	43



# Chapter 1 Introduction

## 1.1 Background

Urbanization has significantly altered the natural landscape, leading to several environmental challenges, one of the most prominent being the Urban Heat Island (UHI) effect (Oke, 1982a). The UHI effect refers to the temperature disparity between urban areas and their surrounding rural regions, primarily caused by the replacement of natural vegetation with impervious surfaces such as asphalt and concrete. This phenomenon exacerbates local climate changes, increases energy consumption, and contributes to deteriorating public health due to extreme heat exposure (Odli et al., 2016).

Among numerous mitigating measures, green roofs have emerged as a viable solution to UHI effects. Green roofs incorporate plants into urban infrastructure, improving temperature regulation through increased evapotranspiration, albedo, and building insulation. According to studies, green roofs can dramatically reduce surface and ambient temperatures, resulting in lower cooling energy consumption and improved urban microclimates. Green roofs substantially reduce sensible heat fluxes released to the outdoor environment, with reductions ranging from 42% to 75% depending on the climate, helps in reducing the peak cooling load of the building as well as lowers the heat rejection rates from the cooling system condensers (Costanzo et al., 2016). Other than these advantages, green roof also helps in stormwater management by absorbing and filtering rainwater, thereby reducing runoff and alleviating pressure on urban drainage systems. Noise reduction and extended roof lifespan by protecting against UV radiation and temperature fluctuation increases property value (Jamei et al., 2021).

Montreal, like many metropolitan areas, is affected by UHI, notably in its heavily populated downtown area. This study uses advanced modeling approaches such as the ENVI-MET software to assess the effectiveness of green roofs in mitigating UHI in the Montreal region. The study examines temperature fluctuations under various scenarios—both with and without green roof installations—during normal and harsh summer temperatures. Furthermore, the study looks at changes in relative humidity and overall thermal comfort to provide a comprehensive assessment of green roofs as a sustainable urban cooling solution.

When it comes to climate change, one of the worst consequences of it are natural disasters. The most common natural disaster that can be seen over years in Montreal is Flooding. The Montreal Island is surrounded by water body from all the sides. Urbanization dramatically raises flood risk by modifying natural hydrological processes, mostly through the spread of impervious surfaces like roads, parking lots, and buildings. This impermeable materials limit water infiltration, leading to greater surface runoff, shorter hydrologic response times, and higher peak discharge rates during rainstorm events (Feng et al., 2021a). Urbanized areas have heightened flood conditions as water rapidly collects, overwhelming current drainage systems and leading to more frequent and severe flooding episodes (Agonafir et al., 2023a). Furthermore, the spatial distribution of impervious surfaces has a significant impact on flooding severity; concentrated urban development can exacerbate flash flood conditions more severely than evenly distributed urbanization, highlighting the importance of spatial planning in mitigating urban flood risks (Feng et al., 2021a).

Furthermore, urbanization is frequently connected with greater economic and social vulnerability, as dense infrastructure and populations heighten the risk of flood-related damage and casualties (Agonafir et al., 2023a).

By integrating GIS-based urban climate classification, microclimate simulations and flood risk mapping, this research aims to support urban planners and policymakers in making informed decisions about sustainable urban development (Dwivedi & Mohan, 2018). The findings add to the broader discussion on climate-resilient cities by illustrating the real benefits of incorporating green infrastructure into urban design, particularly in terms of minimizing urban heat islands and lowering flood risks. This study provides vital insights for effective flood control techniques by analyzing flood-prone zones spatially and the impact of urban land-use patterns, emphasizing the need of integrated planning approaches in developing resilient urban settings.

## **1.2 Problem Statement**

The record-breaking urbanization on the one hand leads to increased development, job opportunity, cultural exchange but on the other hand it leads to altered local landscapes and climate, causing interconnected environmental hazards. The two most critical challenges are Urban Heat Island (UHI) effect and increased frequency and severity of urban flooding. When natural, permeable land cover is replaced with materials that don't let water through, like asphalt and concrete, it changes the balance of energy on the surface, making cities much warmer than the areas around them. This UHI phenomenon not only increases energy use for cooling, but it also puts people's health at risk by making heat-related illnesses and deaths worse (Heaviside et al., 2017).

The rainwater infiltration reduction leads to increased surface runoff which increases the load on the traditional drainage system causing more frequent, intense flooding events, especially as climate change alters precipitation patterns. The city of Montreal is chosen for this study because of its geographical location, being an island makes it more susceptible to flooding. Furthermore, the region is experiencing an intense warming phase since the mean temperature for the past decade was higher, increasing the regional UHI effect and straining the population and the region's infrastructure.

Although nature-based solutions (NBS) such as green roofs are increasingly acknowledged as a valuable tool for climate adaptation, their realization is typically evaluated for one benefit alone, such as thermal regulation or stormwater control (Speak et al., 2013). There is a significant need for an integrated evaluation considering the double purpose of the green roofs for simultaneously controlling both the UHI and the flood risk under the considered urban scenario. There is a significant imbalance regarding the analysis of the spatial interlinkages among the two assessed risks within the city of Montreal and the performance of a large-scale green infrastructure intervention under the variability of the city's urban shapes from the compact high-rise neighborhoods through the extension of the open low-rise districts.

In this study, the mitigation strategy for both the issues is being addressed. Using an integrated methodology that combines both GIS-based flood risk mapping with microclimate simulations in ENVI-MET, this study will help to quantify the results based on city-wide green roof installation

on the temperature and drainage density pattern of the area. The findings aim to provide urban planners and policymakers with the evidence-based spatially explicit insights necessary to strategically implement green infrastructure for a more sustainable and resilient urban future (Demuzere et al., 2014).

### 1.3 Research Questions

This thesis aims to address the following fundamental research questions:

1. How does the installation of green roofs affect the Urban Heat Island effect in the Montreal region?
2. What are the potential environmental benefits associated with large-scale green roof implementation in Montreal?
3. How much can the installation of green roofs change runoff coefficients and hence lower the risk of urban flooding in the Montreal region?
4. How does urbanization affect the spatial distribution and intensity of flood risks, and how does the distribution of impervious surfaces contribute to these risks?
5. What are the spatial links and synergies between urban heat islands and flood risk in Montreal, and how can GIS-based spatial studies help with climate-resilient urban planning?
6. What practical recommendations can spatial analysis and microclimate simulations provide to urban planners and policymakers as they implement effective green infrastructure solutions for climate-resilient urban design?

By addressing these research questions, this thesis aims to provide valuable insights into the potential of green roofs as an effective strategy for mitigating the Urban Heat Island effect in Montreal. The findings from this study will contribute to the broader understanding of sustainable urban planning and climate change adaptation strategies in urban environments.

### 1.4 Thesis Structure

This thesis is divided into four main parts. The first part introduces the background of the study, problem statement and research questions. **Chapter 2** talks about the interconnection between the Urban Heat Island (UHI) and Flood risk in the region. It describes the background literature, how the UHI and Flood affects the urban areas and the mitigation strategy of using green roofs as a solution to both the issues. It shows the effect on green roof installation on the flood risk map for the region. **Chapter 3** shows the methodology to develop the flood risk map of the Montreal region based on GIS and AHP method and introduces the UHI mitigation strategy i.e., installing city wide green roofs and shows its effect on the pedestrian level temperature based on elevation of the surrounding buildings. **Chapter 4** shows the result and interpretation of the observed results **Chapter 5** talks about the conclusion, limitation of the study and the future work recommendation.

## Chapter 2 Background and Literature Review

### 2.1 Urban Heat Island

The Urban Heat Island effect can be defined as the difference in temperature in the urban and the surrounding rural areas. This is especially true at night when there are few clouds and light wind (Douglas et al., 2020). The urban areas observe higher temperature as compared to the rural surrounding areas.

The British scientist Luke Howard was the first one to notice the air temperature in Cities, which was London in this case, is higher than the undeveloped surrounding areas in around 1818 (Roth & Chow, 2012). Since then, other studies have used various stationary or mobile monitoring techniques to explain the spatio-temporal distribution of urban temperatures (Yow, 2007). A more process-based perspective ascribes the genesis of UHI to changes in urbanization-induced energy balance (Oke, 1982), which are governed by changes in urban structure, form, cover, and metabolism.

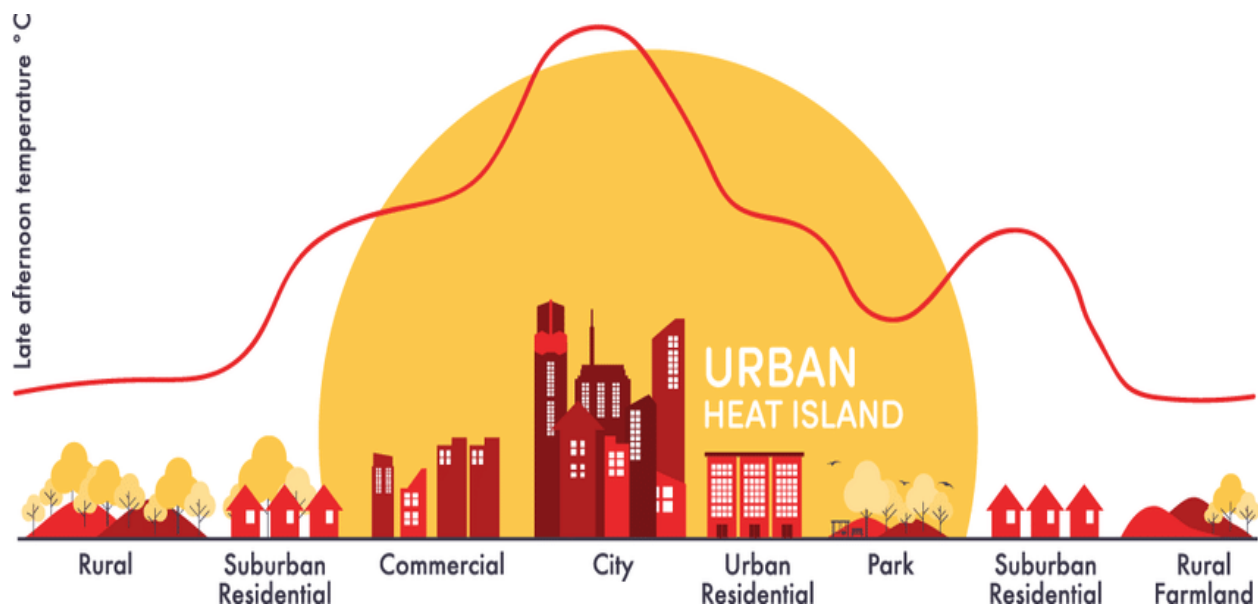


Figure 1. Urban Heat Island (Fuladlu et al., 2018)

Over the years due to rapid urbanization and climate change, the average temperature of Montreal region is increasing. As shown in the graphs below (**Error! Reference source not found.**), it can clearly be seen that the average temperature over the past 12 years has increased by an average of  $0.17^{\circ}\text{C}$  per year, which is significant. There are numerous reasons for this rapid change climate of the area but mainly it's because of the increasing industrialization and urbanization. Due to the

increasing temperature, more energy is consumed to maintain cooler surroundings which ultimately affects the climate of the region.

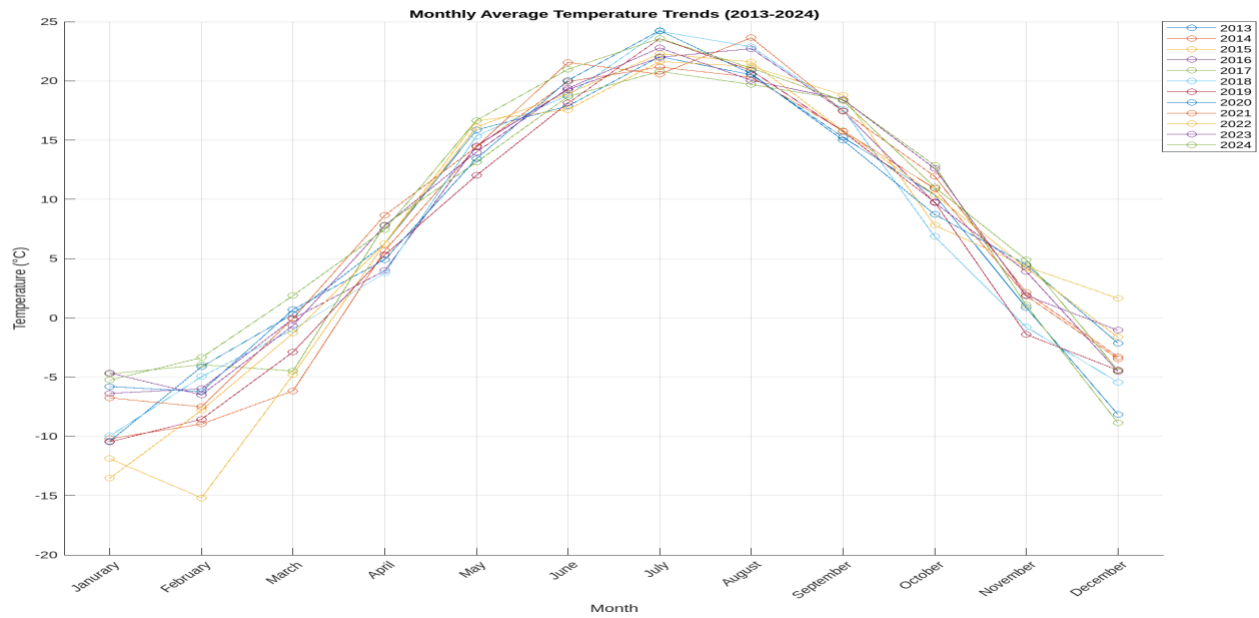


Figure 2. Historical Average Monthly Temperature (2013-2024)

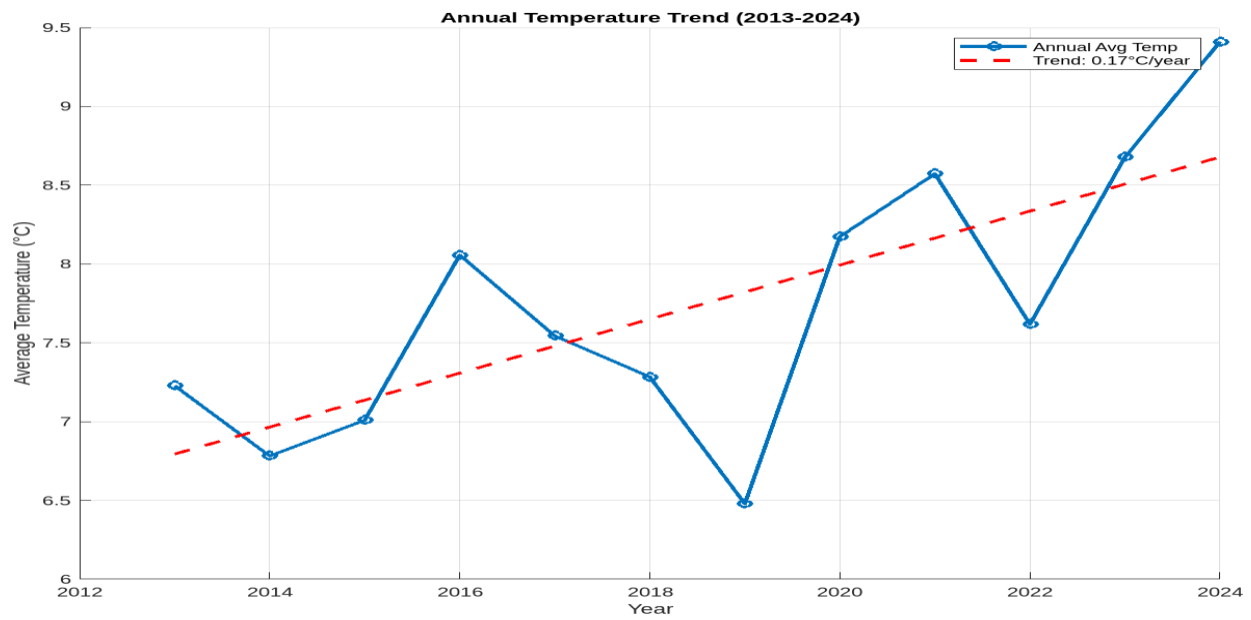


Figure 3. Temperature Trend Over the Year 2013-2024

The graphs shows that the average temperature of the Montreal City is increasing every year.

The consequences of UHI are anticipated to worsen as cities grow, with built-up areas projected to triple in developing countries and increase 2.5 times in developed countries. The effects of UHI will be even more noticeable by 2050, when about 70% of people on Earth will live in cities. (Angel et al., 2005)

### **2.1.1 What causes Urban heat island effect?**

UHI effect is caused by the combination of natural and man-made factors which collectively alters the energy balance in urban areas. The five fundamental factors are anthropogenic heat additions, albedo decrease, storage of heat in infrastructure (buildings, paved areas etc.), evapotranspiration, or variations of energy transfer between the surface and the lower atmosphere. Further, out of these five, two dominant contributors are reduction in evaporative cooling in urban areas and Albedo which refers to the percentage of sunlight or radiation reflected by the surface (L. Zhao et al., 2014). A few factors are explained in detail below:

- **Impervious Surfaces:** Concrete, asphalt, and brick are common materials in urban contexts, which absorb and retain more solar radiation than natural surfaces, resulting in higher temperatures.
- **Reduced Vegetation:** Cities with less vegetation and green areas retain more heat because evapotranspiration, a natural cooling mechanism, is reduced.
- **Waste Heat Emissions:** The urban atmosphere warms by the heat produced by automobiles, factories, and air conditioners.
- **Urban Geometry:** The congested layout of tall buildings results in "urban canyons," which limit natural cooling by trapping heat and reducing wind flow.
- **Air pollution:** Pollutants can change how radiation is absorbed and emitted, which raises temperatures even more.
- **Delayed Cooling:** Compared to rural locations, urban materials tend to release stored heat more slowly during the night, keeping temperatures higher.

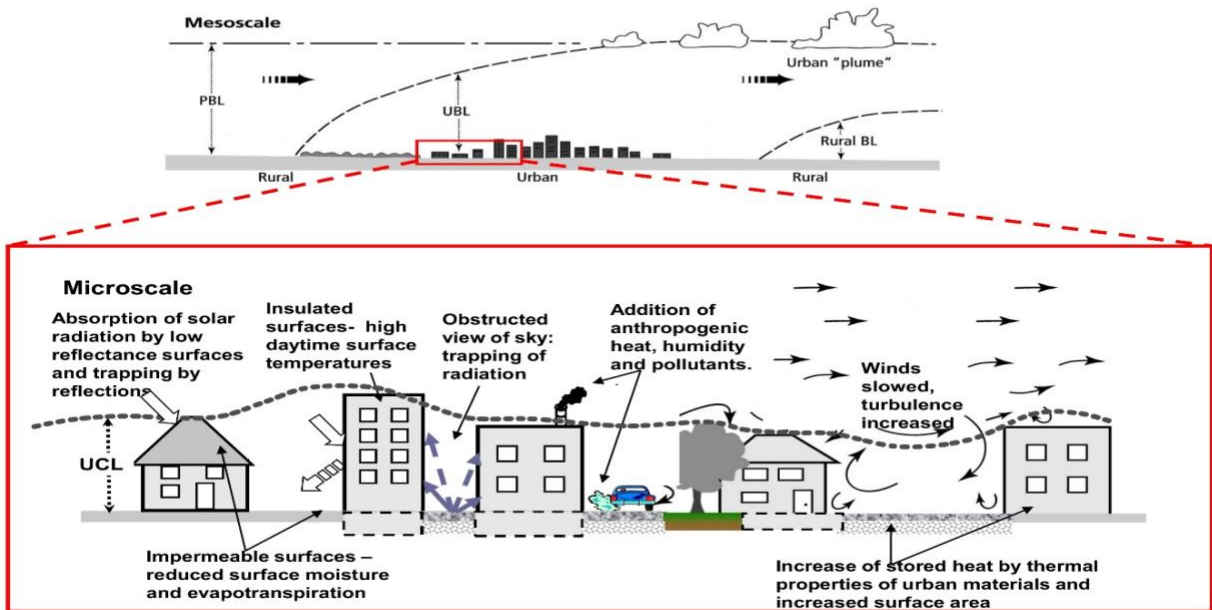


Figure 4. Processes contributing to urban heat islands at regional and microscales (BELHADJ, 2020a)

The figure above has two main parts and shows the causes of urban heat islands at the regional and microscale levels (BELHADJ, 2020a).

The upper portion of the figure depicts the urban heat island effect on the regional, or "mesoscale," level. The urban boundary layer (UBL) in this case stretches over the planetary boundary layer (PBL) and advects downwind, forming a plume of air over a newly forming rural boundary layer (rural BL) (BELHADJ, 2020b).

In the bottom part of the figure, a portion of the urban skyline from the upper diagram is enlarged to show the urban heat island effect at the microscale. Various arrows point out features of the "urban land surface" that lead to urban heat islands. The lower part of the figure discusses that:

- Roof surfaces tend to have low reflectance, absorbing and trapping solar radiation.
- Impermeable surfaces, i.e., roads, restrict surface moisture and diminish evapotranspiration.
- Insulated surfaces can result in hot daytime surface temperatures.
- Densely packed buildings block the sky view, entrapping radiation, retarding wind, and enhancing turbulence.
- Thermal properties of urban materials, such as buildings and roads, and their greater surface area, all add to stored heat.
- Buildings and vehicles emit anthropogenic heat, moisture, and pollutants into the atmosphere.

### 2.1.2 UHI in urban climatology

UHI is critical in urban climatology because it depicts how urbanization fundamentally alters local climatic conditions. Temperatures are often higher in urban areas due to the higher absorptivity of buildings and pavements, as well as the lack of greenery, which limits evaporation and thus evaporative cooling. Urban areas affect the near-surface climate by their effects on energy and water partitioning at the surface due to their distinct thermal, radiative, moisture, and aerodynamic characteristics ((Roberge & Sushama, 2018). Urban canyons can also influence wind speed and cause wind channeling. Air cooling and heating systems, as well as vehicle emissions, are additional anthropogenic elements that can intensify UHI ((Landsberg, 1981).

The UHI is critical in the urban climatology:



*Figure 5. Adverse effects of UHI*

- **Temperature Modification:** Due to UHI, local microclimates are drastically changed, with urban regions experiencing greater temperatures than their rural counterparts.
- **Energy Consumption:** High urban temperatures raise the need for cooling, which increases energy consumption, stressing energy infrastructure.
- **Impacts on Public Health:** Severe heat-related illnesses, increased air pollution, respiratory and cardiovascular problems can all be made worse by rising temperatures.
- **Environmental Effects:** UHI can intensify the production of smog and affect regional weather patterns, such as changes in precipitation and wind patterns.
- **Urban Planning and Sustainability:** Understanding UHI is critical for developing effective mitigation techniques such as green roofs, urban vegetation, and reflecting building materials that will result in more sustainable, resilient communities.

### 2.1.3 Local Climate Zone Classification

The study area chosen for the urban heat island analysis within Montreal is based on local climate zone classification. The classification is based on urban landscapes according to build environment, land cover, and land use feature and was done using ArcGIS Pro.

The classification on the urban area ranges from high density central urban area to lower density suburban areas. These classes cover socioeconomic dynamics, infrastructure concentration, and different architectural typologies (Stewart & Oke, 2012a). They consist of compact high rise (LCZ 1), compact midrise (LCZ 2), compact low rise (LCZ 3), open high rise (LCZ 4), open midrise (LCZ 5), open low rise (LCZ 6), light with low rise (LCZ 7), large low rise (LCZ 8) sparsely built (LCZ 9), and heavy industry (LCZ 10). Complementing this are 7 land cover types, capturing natural and semi-natural environments within urban landscapes. These include green spaces, vegetated areas, bare soil patches, and water bodies that reflect urban ecological diversity. The land cover classes comprise dense trees (LCZ A), scattered trees (LCZ B), bushes and scrubs (LCZ C), bare rock and paved (LCZ D), bare soil and sand (LCZ E), and water (LCZ G) (Bechtel et al., 2020).

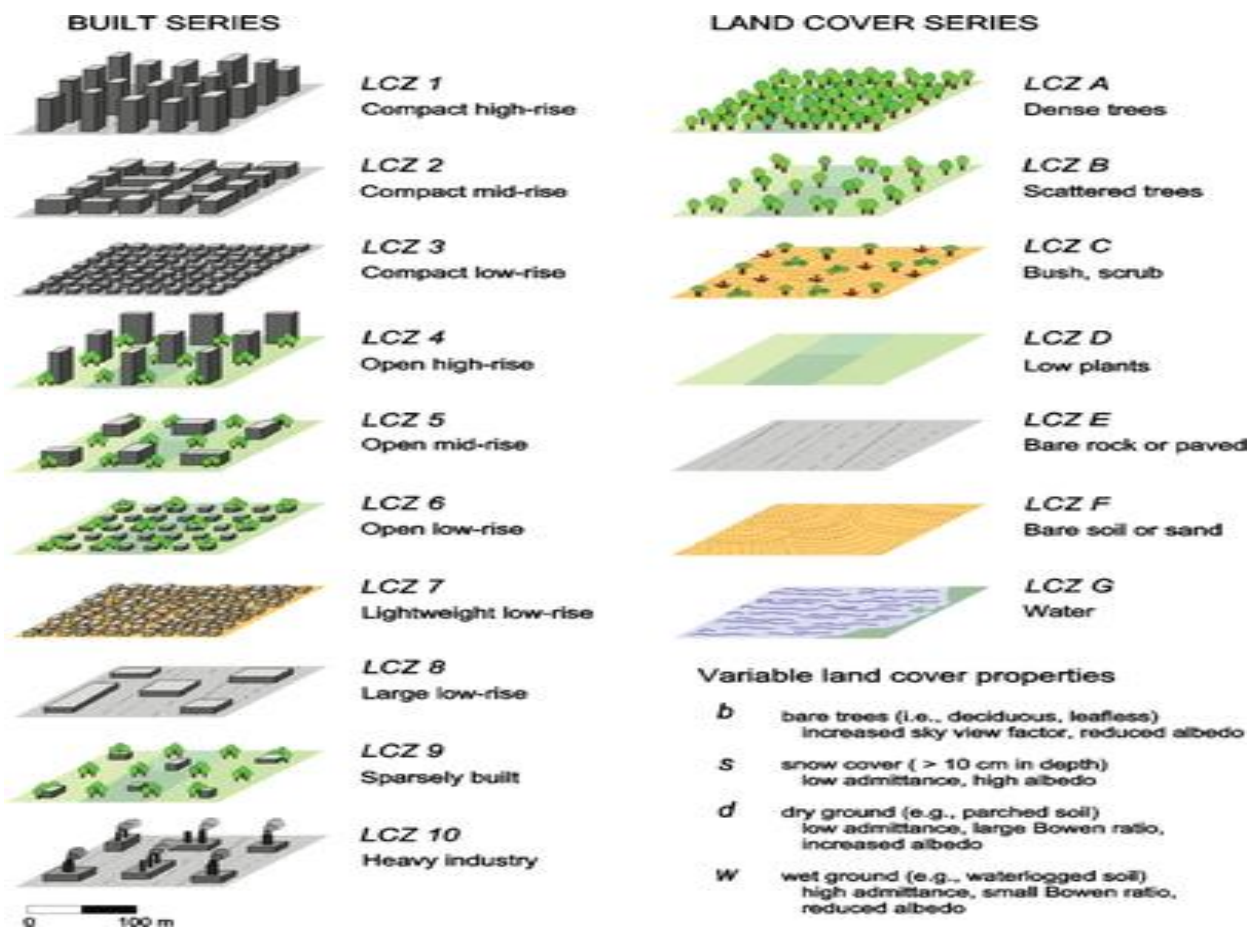


Figure 6. Local Climate Zone classification

#### 2.1.4 Advantages of considering Local Climate Zones:

- LCZ mapping is particularly beneficial for urban climate research, sustainable city planning, and environmental monitoring.

- Researchers can use LCZs with GIS and remote sensing to assess temperature distributions, identify heat-prone locations, and design climate adaptation techniques such as green roofs, more vegetation, and reflective building materials. This approach helps policymakers create cities that are resilient to climate change and provide a consistent foundation for comparing urban climates around the world.
- LCZ mapping aids in increasing urban sustainability, lowering the effects of UHI, and prioritizing places for green infrastructure in cities like Montreal.

### 2.1.5 Mitigation Strategies

There are a few mitigations strategy which significantly affect the UHI of a region. Here, few are discussed below:

- **Ventilation and Air Passage** – Increasing air passage enhancing airflow in urban areas to reduce heat build-up. The study suggests that ventilation and air passage play an important role in minimizing the Urban Heat Island (UHI) impact by allowing airflow across densely constructed environments. The frontal area index (an essential parameter for assessing underlying roughness and analysing urban ventilation corridors (Xu & Gao, 2022) ) is found to be a valuable metric for evaluating urban ventilation; larger values show a negative link with vegetation cover and a positive correlation with building density, height, and heat island severity. The identification of ventilation corridors as primary channels for cooler air to enter urban cores highlights how planned urban planning can improve air circulation and reduce localized heat build-up. Without changing the overall layout, city planners can enhance urban microclimates and lessen the effects of UHI by preserving sufficient ventilation corridors and improving building orientation (Wong et al., 2010).
- **Use of Water in Urban Design** – Most of the studies highlights that building form and site layout directly affect temperature, heat absorption whereas water body providing cooling through evaporation, increased thermal inertia, and heat absorption Whereas, the presence of lakes, rivers, and artificial water features reduces surrounding air temperatures and helps regulate urban microclimates. Furthermore, the microclimate effects of nearby topography—both natural (land, flora, water bodies) and manufactured (buildings, infrastructure)—must be carefully studied, since disregarding them may result in unsuccessful mitigation attempts. This implies that although water bodies may help reduce UHI, their efficacy varies greatly depending on the context and should be incorporated within a more comprehensive, carefully designed urban planning approach (O'Malley et al., 2014).
- **External Use of High-Albedo Materials** – This is basically applying reflective materials on buildings and pavements to reduce heat absorption. Urban materials are generally darker and possess a higher heat capacity than vegetation (Hayes et al., 2022a). As a result, they absorb and retain more solar energy than their surrounding areas. The way this energy is managed depends on the surface exposed—some of it is conducted through building facades into conditioned spaces, while the rest is released back into the urban environment through radiation and convection, as illustrated in figure below (Hayes et al., 2022b).

According to studies, using high albedo coatings can lower pavement surface temperatures by 15°C when compared to conventional materials (Zhu & Mai, 2019). But there are drawbacks, such as glare, expense, and the possibility of unwanted heating effects from reflected sunlight on surrounding structures. A crucial UHI mitigation strategy, particularly in hot metropolitan areas, is the use of reflective pavements and other high albedo materials. Their incorporation into urban planning can enhance thermal comfort, lessen extreme temperatures, and promote sustainable urban growth.

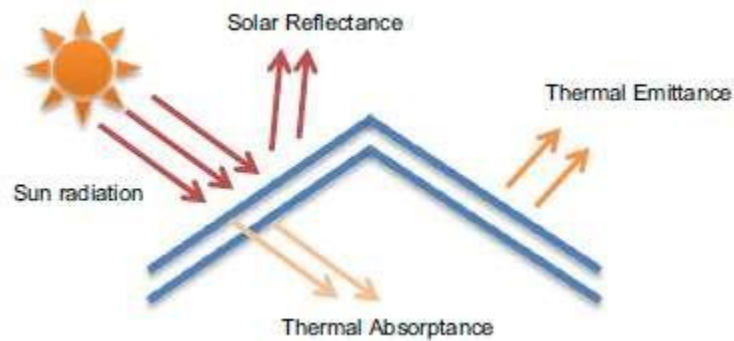


Figure 7. Schematic of roofing surfaces subject to incident solar energy (Al-Obaidi et al., 2014)

- **Presence of Green roofs and Green Spaces** – Green roofs, also known as eco-roofs, roof gardens, vegetated roofs, are a system in which vegetation is cultivated within a specialized growth medium or substrate. The choice of materials and the arrangement of components in a green roof determine how the system interacts with local climate conditions and precipitation. Green roofs are commonly categorized based on their structural composition, falling into three main types: intensive, semi-intensive, and extensive as shown in figure below.

Green roofs can be segmented into three classes, differentiated according to their substrate thickness, selection of plants, as well as their level of maintenance. Intensive green roofs sustain a wide variety of plants ranging from grasses, through shrubs, to even trees, usually requiring more than 25 cm of soil. Frequent maintenance is required in these systems, involving irrigation, fertilization, as well as ongoing plant maintenance. Extensive green roofs, conversely, consist of drought-tolerant plants like grasses as well as herbs, supported by a thinner substrate of 8 to 15 cm thickness. They require minimal irrigation as well as low levels of maintenance. A midway point is the provision of the semi-intensive green roof with the use of small bushes as well as grass with 15 to 25 cm substrate thickness. Although more demanding compared to extensive green roofs, their level of maintenance is less compared to a fully intensive system. Of these, extensive green roofs have the widest use because of their light structure, simplicity of fixing, as well as low irrigation

requirements, factors which collectively contribute to their low-cost as well as low-maintenance attributes (Hayes et al., 2022b).

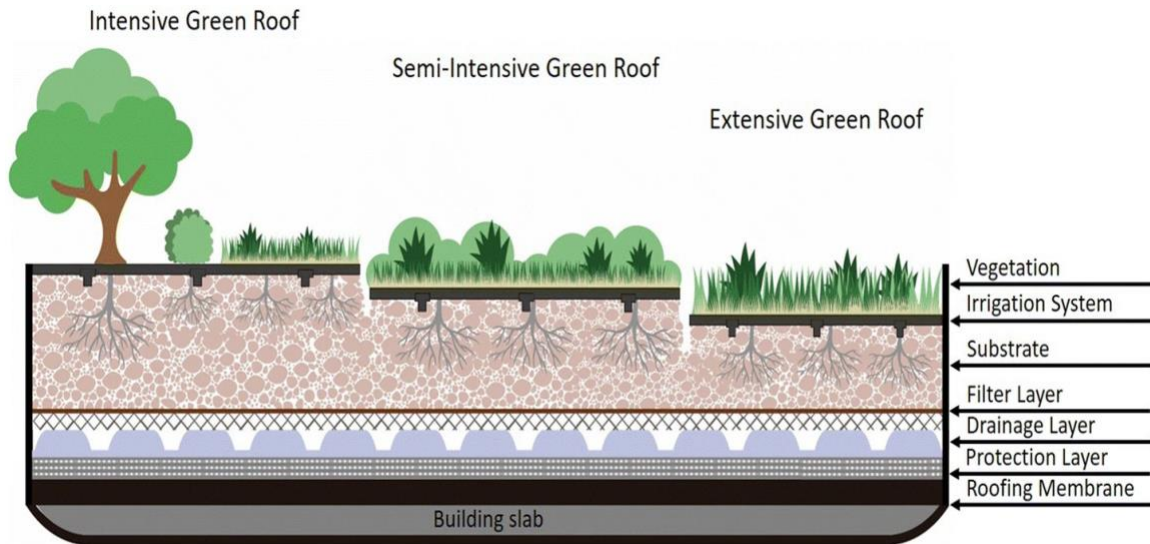


Figure 8. Types of Green roof system and typical components (Calheiros & Stefanakis, 2021)

On the other hand, Urban green spaces are defined as the interconnected network of natural or developed green spaces dispersed throughout an urban territory. Its purpose is to increase the overall vegetation index of the city. Green spaces include vegetation along transportation routes, public gardens, on private lands e.g., residential, commercial and industrial buildings (Urban Heat Island Mitigation Strategies: 2021 Update November 2021 Synthesis Of Knowledge, N.D.). Studies show that green spaces in dense high-rise buildings can reduce upto  $1.05^{\circ}\text{C}$  (Kim et al., 2025) due to the shading effect of the high-rise buildings and the regulation of transpiration of green area during heat waves. More specifically, the shading from the tall buildings precludes the reduction of transpiration of green plants under the sun, maintaining the evaporative cooling benefit of green areas under a heat wave. But at night there is no shading, leaving only the evaporative cooling benefit of green areas (Kim et al., 2025).

### 2.1.6 Urban Heat Island classification Montreal

The heat island in Montreal which represents five classes Freshness Island, Colder than average temperatures, temperature closer to average, temperature warmer than average temperatures and

Heat Island that is very high temperature (*Vulnérabilité Aux Aléas Climatiques de l'agglomération de Montréal, n.d.*).

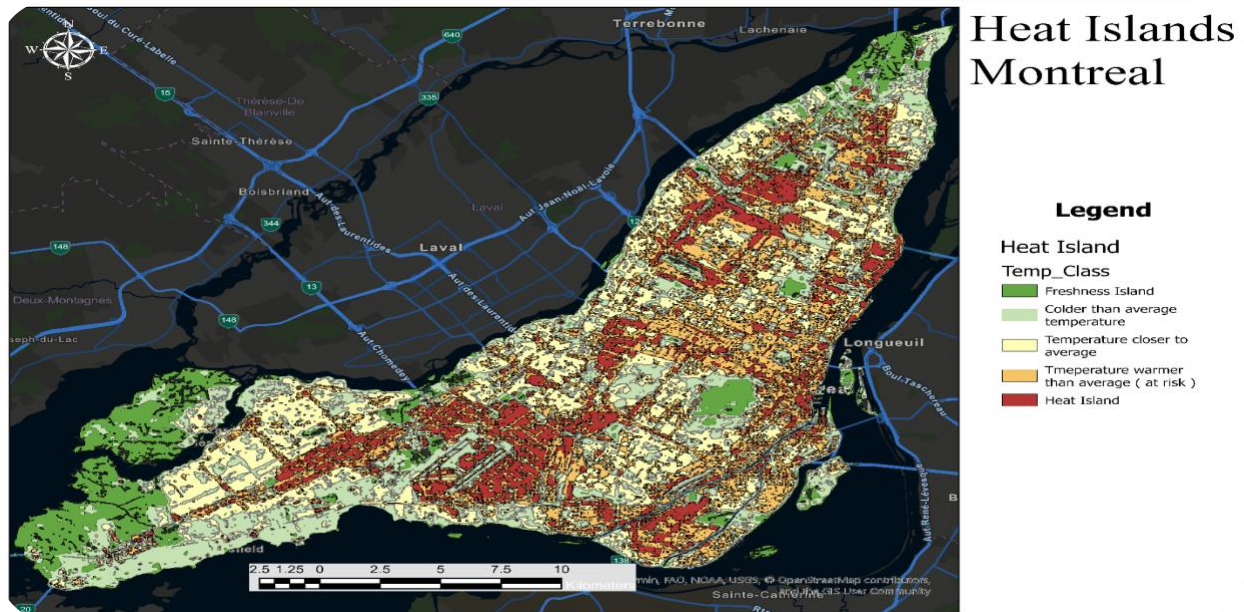


Figure 9. UHI Montreal

**2.1.7 Link to Green Roofs:**

In line with the mitigation measures earlier discussed to address the Urban Heat Island (UHI) effect, green roofs are among the most promising countermeasures. Green roof cools the environment by providing shade, evapotranspiration, and thermal insulation through the introduction of vegetation on rooftops. (Shafique et al., 2018) Not only do these processes reduce surface and ambient temperatures, but they also complement other urban greening efforts, such as tree canopies and green spaces, by extending their cooling effects to building surfaces. Studies show that it can reduce the heat flow through roof by 70-90% in summer and 10-30% in the winter (Liu & Minor, n.d.). Green roofs are thus essential towards creating a more sustainable and heat-resilient urban environment. In this study, green roofs are introduced in the study area and Envi-Met is used simulate the scenario and measure the effect of green roofs on UHI of the region.

**2.2 Urban Flood Risk Assessment**

As a key purpose of conducting flood risk assessment is to support the development of effective management strategies to reduce the overall risk of flooding, the identified flood risk areas in different levels will be illustrated on flood risk maps using GIS. This will offer a clear visualization to assist in risk communication and decision making for future flood risk management. The next subsections provide detailed explanations about flood risk mapping by different aspects. The

vulnerability assessment aims to identify the susceptible locations to flood events and the populations or elements at risk. Vulnerability in this study refers to the potential for damage and is classified as a physical or social vulnerability. Social vulnerability highlights the ability of people in a community to anticipate, prepare for, and respond to hazards, whereas physical vulnerability refers to the potential for physical damage. Vulnerability assessment involves seeking and identifying vulnerable elements and populations at risk, as well as their level of vulnerability. This type of assessment allows policymakers and planners to pinpoint priorities and develop appropriate plans to improve public safety and reduce physical and social risks associated with flooding. The study is specifically focused on the flood risk in Montreal due to climate change. The research closely investigates two levels of flood risk assessment: flood hazard mapping and vulnerability assessment. Flood hazard mapping is a crucial part of flood risk assessment. It provides critical information for spatial planning and urban development, as well as mitigating measures for flooding. The findings of a flood hazard assessment can be utilised to make better decisions on land use and development by avoiding and preventing flood hazards (Kumar & Jha, 2023).

### **2.2.1 Flood Risk Exacerbation by Climate Change**

Climate change has exacerbated urban flooding by altering precipitation patterns and increasing storm frequency and intensity. Urban areas are especially vulnerable because of their low infiltration capacity, as impervious surfaces accelerate runoff generation, creating conditions conducive to flash floods (Agonafir et al., 2023b). Climate change-driven increases in temperatures and changing rainfall distributions have amplified heavy rainfall events, aggravating urban flood threats around the world. Furthermore, forecasts show that flood frequency will continue to rise, particularly in metropolitan areas, which makes it necessary to take the adaptation methods as part of urban design to effectively manage future risk (Yin et al., 2015).

### **2.2.2 Role of Urbanization and Land-Use Changes**

Urbanization has a substantial impact on flood dynamics because it increases impervious surfaces such as highways, rooftops, and parking lots, which disrupts natural hydrological cycles. This development reduces the urban landscapes' ability to absorb water, resulting in increased runoff and shorter response times during heavy rainfall events (Feng et al., 2021b). The spatial distribution patterns of impervious surfaces have a major impact on flood severity, implying that densely packed urban growth increases flood risk more than equally distributed impervious surfaces. Furthermore, uncontrolled urban development and land-use alterations aggravate socioeconomic vulnerabilities by locating key infrastructure and inhabitants in flood-prone areas (Moscrip & Montgomery, 1997).

## **2.3 Synergies between Urban Heat and Flood Risks**

Flooding and urban heat islands (UHI) are related climate hazards that frequently co-occur in crowded urban areas. Urban residents suffer increased dangers because of the developed environments' replacement of natural vegetation, which raises surface temperatures and surface

runoff (Rahman et al., 2021). The synergistic connections between UHI and urban flooding highlight the importance of implementing integrated mitigation strategies, such as green infrastructure, to address various urban climate risks at the same time (Pathirana et al., 2014). Furthermore, green roofs modify urban hydrology by increasing water retention and infiltration capacity, resulting in lower runoff coefficients. These dual benefits contribute to flood risk reduction by lowering runoff volumes and peak discharge rates during storm events, making them important components of urban climate adaptation measures (Huang et al., 2017).

## **2.4 State-of-the-Art: UHI and Flood Mapping**

Urban regions all over the world now suffer from interrelated climatic hazards, namely the Urban Heat Island (UHI) phenomenon and periodic flooding events. Accordingly, suites of cutting-edge measurement and mapping techniques have been established throughout the world. A review of these methods provides the necessary context to situate the methodological contributions of this thesis.

### **2.4.1 Global Approaches to Urban Heat Island (UHI) Assessment**

UHI evaluation is an established urban climatology practice, and various standardized techniques are used internationally. The dominant method is using satellite thermal remote sensing. Thermal sensors onboard satellites such as Landsat and MODIS provide data used for extracting Land Surface Temperature (LST), thus offering a spatially overall picture of heat distribution, and facilitating the obvious detection of urban hotspots (Weng, 2009). This technique is foundational to UHI studies in countless cities around the world.

To normalize comparisons of the urban thermal environment, the Local Climate Zone (LCZ) classification was established (Stewart & Oke, 2012a). For high resolution analysis, microclimate models that employ computational fluid dynamics (CFD), such as ENVI-MET, are commonly used. They model the intricate interactions of buildings, vegetation, and the atmosphere, and enable planners to test selected urban designs and mitigation strategies such as green infrastructure prior to implementation.

### **2.4.2 Global Approaches to Urban Flood Risk Assessment**

Methodologies for defining urban flood risk have changed significantly, shifting from the use of historic information to using predictive model methods. Regulatory flood hazard maps have been used in many industrial nations for urban planning and insurance policies. They are typically generated using sophisticated hydraulic and hydrologic model programs (e.g., HEC-RAS, SWMM) that simulate flood extent and depth for selected, significant storm events, for example, the "1-in-100-year" flood occurrence (Teng et al., 2017).

In the context of academic research, specifically in proposing susceptibility maps, the use of GIS-based Multi-Criteria Decision Analysis (MCDA) is identified as a highly popular approach at the international level. Methods such as the Analytic Hierarchy Process (AHP) ensure the ordered consideration and combination of numerous geospatial variables—covering elevation, slope, land

use, and distance to drainage channels—in identifying flooding-susceptible areas. This approach is valued for its coherent framework and versatility in varying geographic conditions (Tehrany et al., 2014). More recently, machine learning algorithms have been gaining significant traction in the subject, which use vast datasets to predict flood susceptibility with high accuracy (Mosavi et al., 2018).

### 2.4.3 Identifying the Research Gap

The methods previously used became more complex and detailed with time, but all practises reveal a persistent research gap which are addressed in this thesis.

- Lack of Integrated Risk Assessment: UHI and Flood risk are studied separately despite broad understanding that green infrastructure has co-benefits, both municipal and academic research. In this study both the factors are combined and quantify the effect of mitigation strategy on both the UHI and the flood risk.
- City Wide Modelling: Many existing maps are static; they identify current problem areas but do not dynamically model the city-wide impact of a specific, large-scale mitigation strategy. The shift from *problem mapping* to *solution-oriented analysis* is a critical and still-developing area of research.
- Case study specific: There is no data available for Montreal region regarding high resolution flood risk map and urban green roof micro-climate simulation for pedestrian comfort. The strategic combination of a GIS-based MCA for macro-level flood risk with high-resolution microclimate modeling for thermal benefits represents a comprehensive and novel approach that is not yet commonplace in urban climate resilience studies.

## Chapter 3 Methodology

The methodology adopted in this study is composed three different parts. The overall process and the structure are described in the Figure-10.

- Developing the flood risk map for the Montreal region.
- Micro-climate simulation to determine the pedestrian level temperature.
- Combining both the studies to compare effects of City-wide green roof installation.

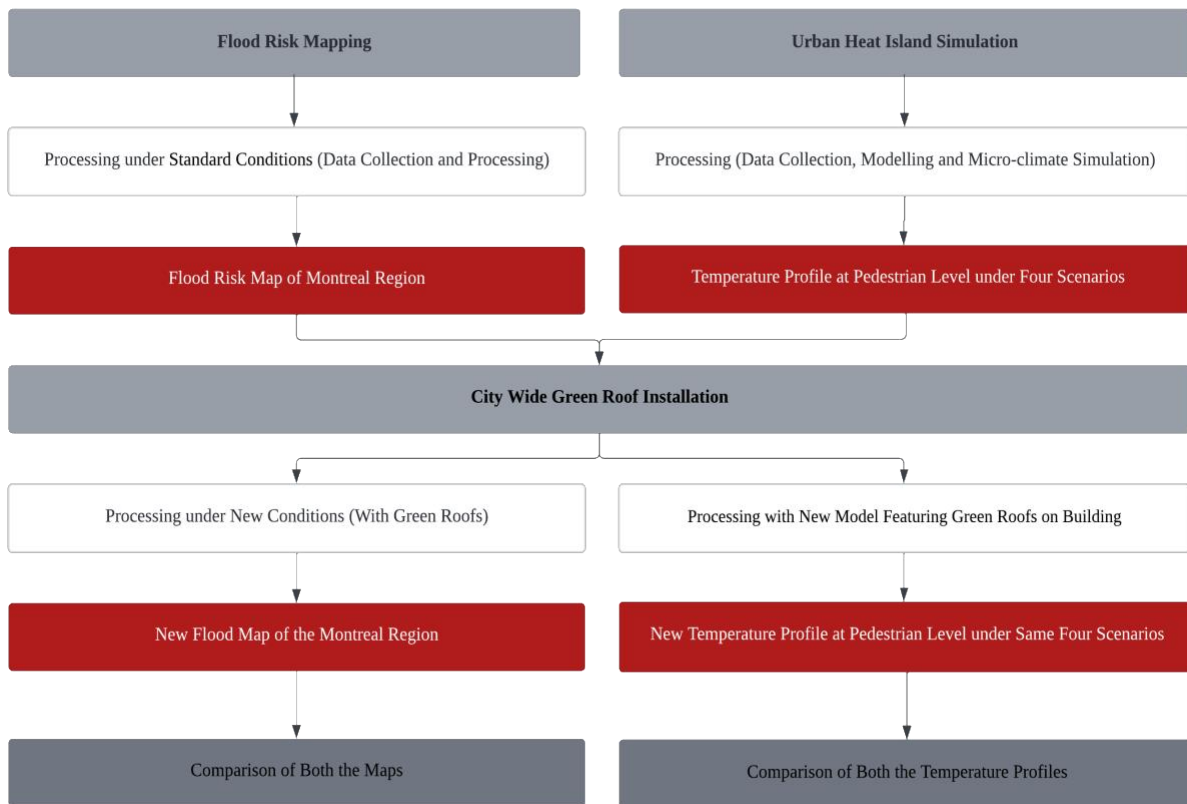


*Figure 10: Overall Thesis Structure*

### 3.1 Flood Risk Mapping

This chapter explains the methodological framework employed to create an extensive flood risk map for the Montreal area. The method combines the Analytic Hierarchy Process (AHP) for multi-criteria decision making and weighting of flood susceptibility factors with Geographic Information Systems (GIS) for spatial analysis and visualization. This approach uses GIS's ability to handle a variety of spatial datasets and AHP's structured evaluation capabilities allow for an open, repeatable, and fact-based evaluation of flood risk in intricate urban settings.

The city of Montreal, located in the province of Quebec, Canada, is chosen as the study area due to its location, history of frequent flooding. Montreal's unusual geographical location between the Ottawa and St. Lawrence Rivers, along with widespread urbanization, makes it especially vulnerable to flooding. This region has already seen multiple large flood occurrences, resulting in significant infrastructure damage and community disruption. Growing urbanization, as seen by increased impervious surface coverage, exacerbates flooding by modifying natural hydrological processes, increasing runoff volumes, and diminishing natural infiltration capacities (Papaioannou et al., 2015).

The tool used in this study is ArcGIS pro. Geographic Information System (GIS) data were gathered from several sources given in the table below. The key datasets acquired include:

Table 1. Data Sources for the raw GIS data

<b>Data</b>	<b>Source</b>	<b>Relevance</b>
Elevation data	Statistics Canada, Environment, Energy and Transportation Statistics Division, 2016, special tabulation of data from Natural Resources Canada (NRCan), Canada Centre for Remote Sensing (CCRS), DEM Montreal	Generation of Elevation data for Montreal
Rainfall data (50 Years)	<a href="#">Historical Climate Data - Climate - Environment and Climate Change Canada (meteo.gc.ca)</a> , <a href="#">CanESM5 Satellite</a>	Generation of Annual precipitation layer
Distance to Stream	<a href="#">LANDSAT8</a> <a href="https://www.google.com/intl/fr/earth/about/">https://www.google.com/intl/fr/earth/about/</a>	Generation of distance to Stream layer
Drainage density	<a href="#">High Resolution Digital Elevation Model (HRDEM) - CanElevation Series - Open Government Portal (canada.ca)</a>	Generation of elevation and drainage density layer

The Flow chart for the methodology:

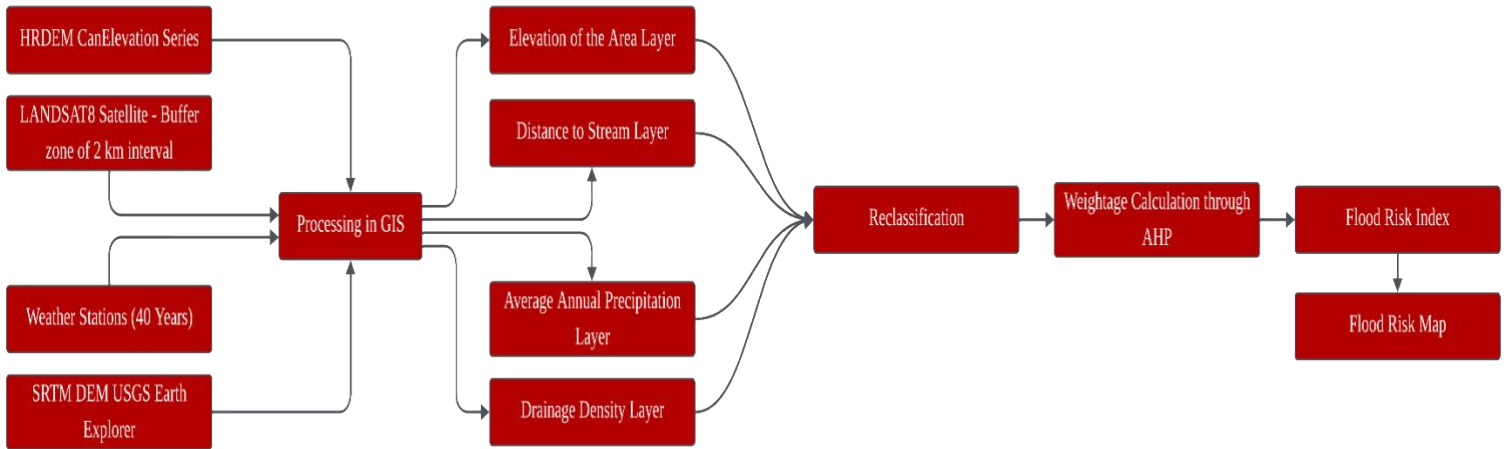


Figure 11: Methodology for Flood Risk Mapping

### 3.1.1 Analytical Framework and Criteria Selection

The analytical framework supporting the flood risk assessment is described in this section, along with the criteria and sub-criteria used for assessing flood susceptibility.

In Montreal, four key factors were found to be significant factors of flood vulnerability:

- Drainage density:** The first step in this procedure is to download Shuttle Radar Topography Mission (SRTM) Digital Elevation Model (DEM) data from USGS Earth Explorer. The raw data is then processed in ArcGIS Pro to delineate the specific boundaries of the study area. All the regions outside the study area were clipped and removed to ensure that the dataset represent only the targeted area. In order to ensure continuous flow, the Fill tool is used to eliminate sinks, or artificial depressions, by raising cells to match the lowest surrounding elevation. The D8 algorithm is then used to create the Flow Direction raster, which gives each cell a downslope direction toward its steepest neighboring cell, encoded in powers of two (1–128). The total number of upstream contributing cells for each cell is then determined by the Flow Accumulation tool:

$$\text{Accumulation}(Z) = \sum_{\eta \in \text{Upstream}(Z)} [\text{Accumulation}(\eta) + 1]$$

The Raster Calculator isolates prominent channels by applying a threshold (Flow Accumulation >10,000) to extract main streams. After that, the binary raster is transformed into polylines using Raster to Polyline and clipped to the edge of the study area. A drainage

density map, which is useful for runoff and erosion analysis, is produced by this workflow; a higher density denotes more concentrated stream networks.

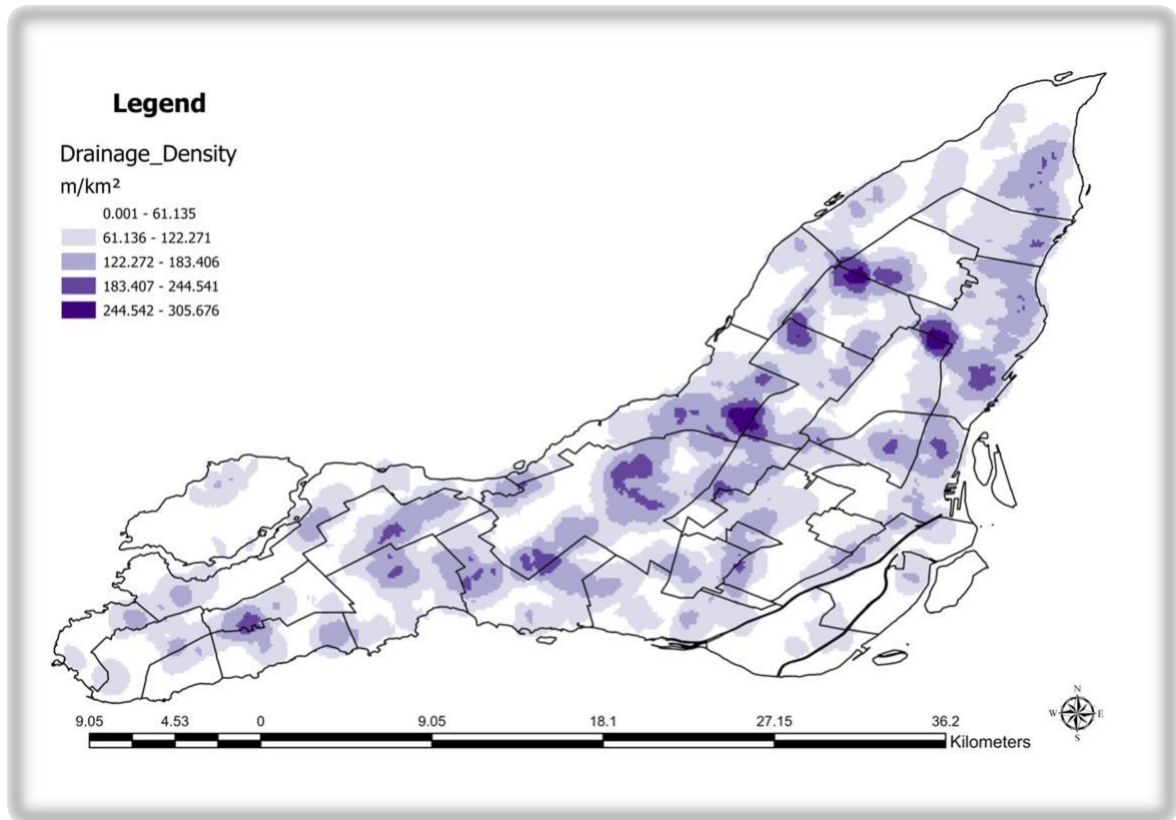


*Figure 12. Drainage Density Layer*

- **Annual Precipitation:** Rainfall data ranging over 40 years (1984 – 2024) is obtained in the NetCDF format. Then the data is cleaned and processed using MATLAB, the data is then converted into format acceptable in ArcGIS Pro. It is then loaded into ArcGIS Pro creating raster layers for each year. After the raster's are combined into a composite raster catalog, monthly rainfall is combined into annual totals per cell. Raster to Point creates point features with rainfall attributes by converting the annual raster to points. A continuous rainfall surface is produced by an Inverse Distance Weighting (IDW) interpolation. Lastly, a map of the annual rainfall is created by symbolizing and composing the interpolated raster.

The spatial variations observed in the below average annual precipitation map are not practically expected given the region's small spatial size, low topography relief, and predominance of large-scale synoptic weather systems. The apparent north-south contrast is due to the data-processing and methodological factors, such as the downscaling and interpolation of coarse-resolution climate model outputs, potential biases resulting from uneven observational station influence, and the cumulative effects of temporal aggregation

and unit conversion. Furthermore, relatively tiny numerical differences may be visually exaggerated when discrete classification intervals are used.

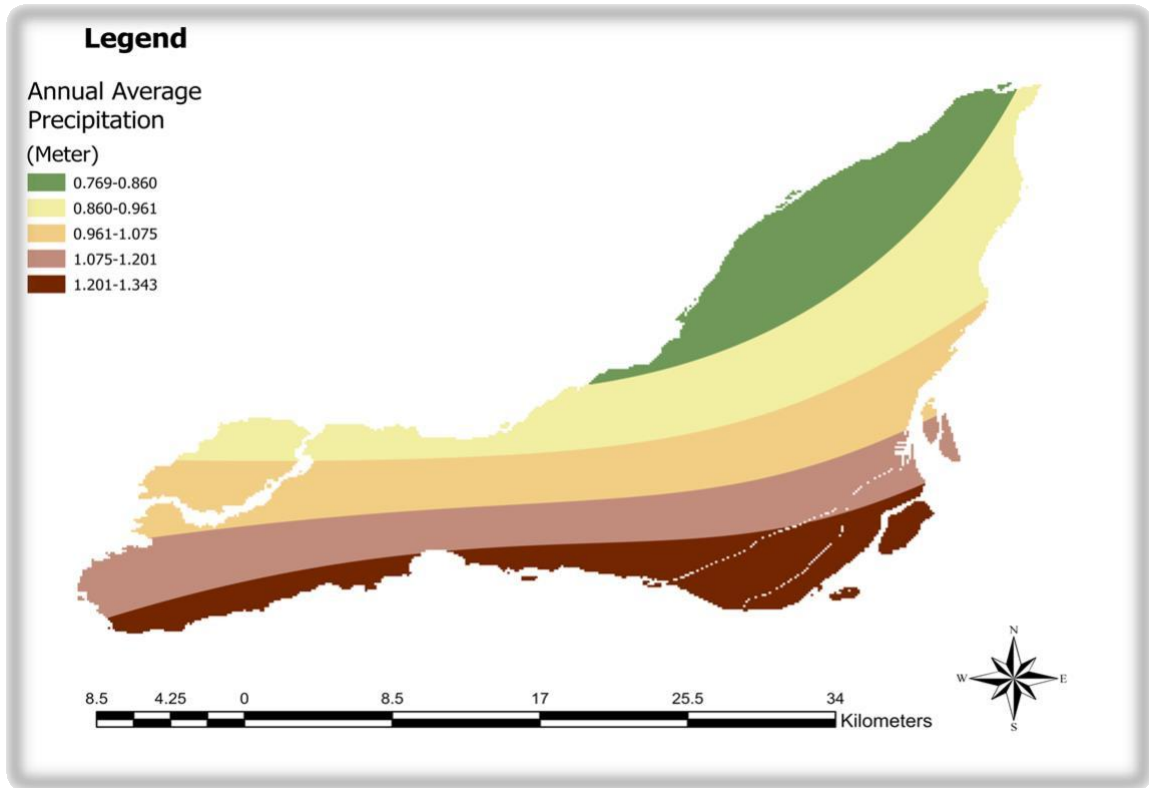


*Figure 13. Annual Precipitation Layer*

- **Distance to Streams:** In order to ensure hydrological continuity, the workflow starts with importing a Digital Elevation Model (DEM) and using the Fill tool to eliminate sinks by adjusting the elevation of each depression cell to match the lowest pour point elevation. The D8 algorithm, which encodes downslope flow directions toward the steepest neighbor based on the gradient slope, is then used to create a Flow Direction raster. In order to create a binary raster, a threshold is applied using Raster Calculator to extract major streams where Flow Accumulation  $>25,000$ . The drainage network file is created by converting raster streams to vector polylines using the Stream to Feature tool after the Stream Link tool uniquely labels connected stream segments to associate stream cells with flow direction.

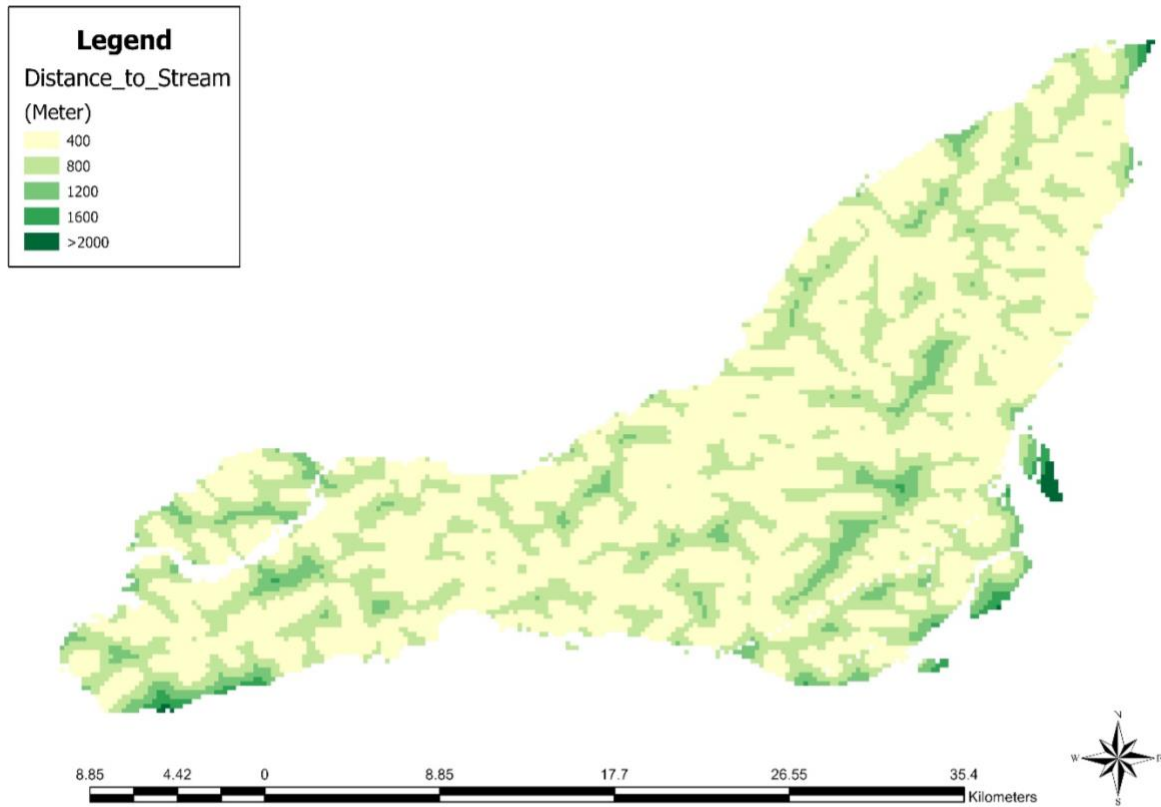


*Figure 14. Distance to Stream Layer*

The drainage network polylines are then surrounded by concentric buffer zones that are created by the Multiple Ring Buffer tool at intervals of 250, 500, 750, and 1,000 meters. In order to enable proximity analysis with respect to the extracted drainage network, the Euclidean Distance tool creates a raster in which each cell contains the straight-line distance to the closest stream segment.

$$d(x, y) = \sqrt{(x - x_s)^2 + (y - y_s)^2}$$

- **Elevation:** This dataset, sourced from DEM file for Canada region gives the information about the topography of the area. This layer provides the elevation details of different region found in Montreal region

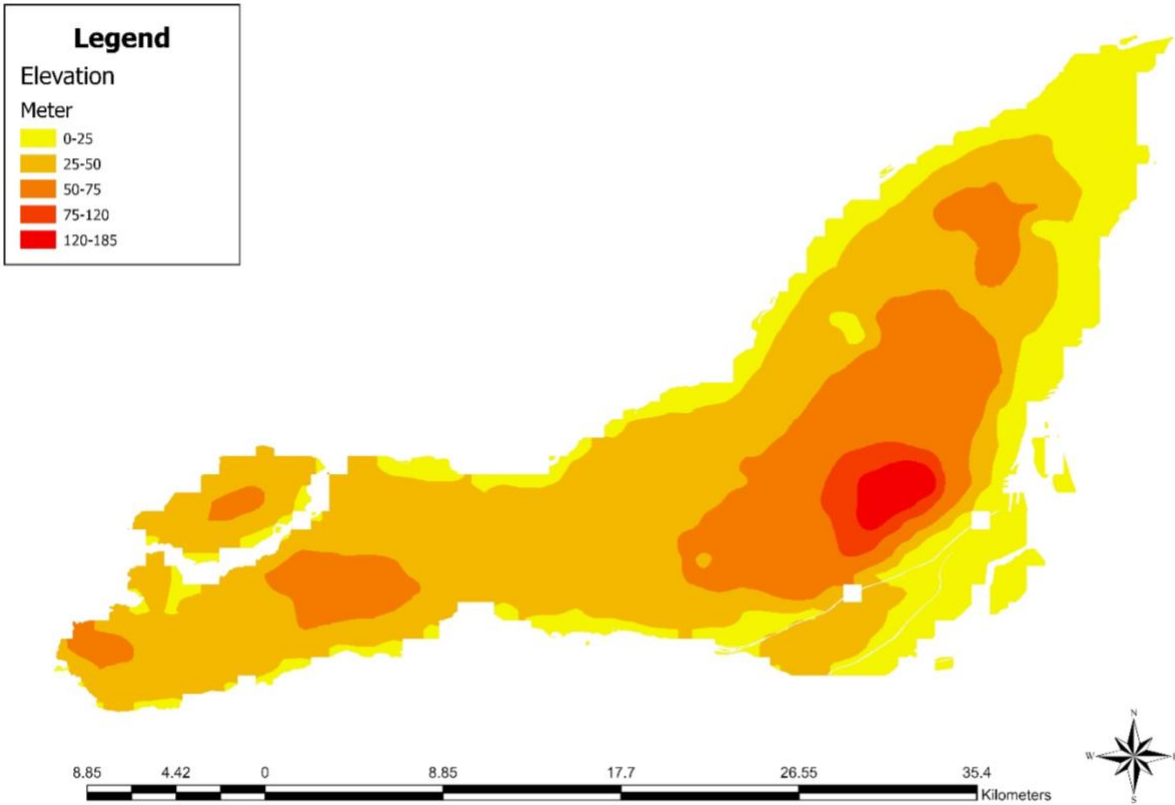


Figure 15. Elevation Layer

Each criterion was operationalized as a spatial layer in GIS, ensuring comparability across data sources and scales. The inclusion of these factors reflects empirical findings from prior flood events in Montreal and is consistent with multi-criteria flood risk studies globally (Khosravi et al., 2016; Mokhtari et al., 2023).

### 3.1.2 Weighting and Consistency Evaluation

Given that flood risk is multifaceted, a systematic weighting process was required to determine the relative importance of each criterion. Because of its extensive use in environmental risk assessments and methodological rigor, the AHP was chosen for this purpose.

### 3.1.3 The Analytic Hierarchy Process

AHP is an effective and simple method in multi criteria decision making process thus, it is used in many industries like engineering, business, finance. The first step consists of defining the decision process. The second step, each parameter zone has been categorized based on its relative importance, according to the Saaty scale (*The Analytic Hierarchy Process*, n.d.). The scale for the relative relevance score was 1 to 9, where lower scores indicated aspects that were less critical and higher scores indicated factors that were significantly more important. It is displayed using a

5x5 matrix with diagonal elements equal to 1 for the pairwise comparison matrix. The values of each row and each column are compared in order to determine the rating score (Abedini et al., 2018; Ameri et al., 2018; Büchele et al., 2006; Fernández et al., 2010; Kantiranis et al., 2015; Khosravi et al., 2019; Mokhtari et al., 2023; Samanta & Koloa, n.d.; Tang et al., 2018; G. Zhao et al., 2018). The normalized matrix is obtained when each column in the comparison matrix summed, and each element is divided by the obtained column sum. The weight factor is the average of each row of the normalized matrix (M. C. Aydin & Sevgi Birincioglu, 2022).

The table to rate the score for each layer is given below:

Table 2. Score Index (*The Analytic Hierarchy Process*, n.d.)

RATING	DESCRIPTION
1	Equally Preferred
3	Moderately Preferred
5	Strongly Preferred
7	Very Strongly Preferred
9	Extremely Strongly Preferred
Values 2, 4, 6, or 8 represent preferences halfway between the integers on either side	

The last step is to verify the consistency of the matrix as the pairwise comparison may not be accurate. It is verified by the below consistency ratio (CR) (Wang et al., 2008) :

$$CR = \frac{CI}{RI}$$

where CI is the consistency index and RI is the random inconsistency index.

$$CI = \frac{(\lambda_{\max} - n)}{(n-1)}$$

Where  $\lambda_{\max}$  eigenvalue and n is the criteria number.

CR must be less than or equal to 0.1 for the matrix to be in the acceptable consistency. The process is repeated until required CR is achieved (Nsangou et al., 2022). After all the calculation, the weighing percent for each layer is found in the table below.

Table 3. Layer Weightage

Layer	Weightage (%)
Elevation	40.31
Annual Precipitation	23.16
Drainage Density	13.38
Distance to Stream	23.15

After calculating the weighing percent, the layers are merged using the ArcGIS tool to get the resultant Flood risk map showing the different areas susceptible to different flood intensity. (ENGINEERING HYDROLOGY Fourth Edition, n.d.).

### 3.1.4 Base Line Flood Risk Map Generation

In this stage, the Weighted Overlay tool in ArcGIS Pro was used to integrate the weighted layers. This tool creates a continuous flood risk index for the entire study area by combining the standardized, weighted inputs.

#### Aggregation Process:

The following formula was used in the overlay analysis:

$$Flood\ Risk\ Index = \sum_{i=1}^n (W_i \times S_i)$$

Where  $W_i$  is weight of criterion  $i$  and  $S_i$  is the standardized score of criteria  $i$  for each raster cell.

Using the natural breaks (Jenks) method, the resulting composite raster was categorized into distinct risk zones (Very Low, Low, Moderate, High, and Very High). This classification facilitated targeted risk communication and enhanced interpretability.

## 3.2 Green Roof Scenario Methodology

Now, we will study what will be the effect of vegetation on the flood risk hot spots. Since we used green roofs as a mitigation strategy for the UHI, it will change the physical characteristics as well as the geographical factors of the area. It will change the insulation of the buildings, increase rainwater retention, absorb pollutants i.e., cleans surrounding air, increase oxygen levels, provide biodiversity, helps in noise insulation, increase property value as it adds aesthetics to the building (Sun et al., 2025). [The factor we have focused on this study is the delayed runoff, reduces peak flow and ultimately changes in the drainage pattern.](#)

Urban areas worldwide face the challenge of climate change and rapid urbanization, which increase the frequency and severity of the urban flooding. In urban areas, most of the surface is

impermeable made up of asphalt, concrete which affects the natural hydrological cycle by reducing the infiltration, evapotranspiration and ground water recharge (Kachholz et al., 2021). In case of excessive rainfall or rapid flood, the drainage network and sewer system are not designed for such high volume of water or peak flow rate which leads to no other option than flooding and property damage. Thus, to reduce this peak flow, NBS or green infrastructure (GI) are proposed to manage the stormwater runoff and reduce the peak flow. This method focuses on the “source control” as green roofs are designed to restore the nature water cycle by absorbing, retaining, and delaying storm water which caused reduced volume of water to enter city drainage systems and lowers peak flow rates during storm.

The main objective is to quantify the hydrological efficacy of city-wide green roof implementation. The analysis will help the urban planners to alter the regional flood risk landscape, provide suitable planning for Montreal’s flood management strategy.

Multiple studies shows that green roof and vegetation decreases stormwater runoff volume ranging from 30% to 90% and peak flow rate ranging from multiple studies show a wide range of efficacy (*Green Roofs & Storm Water Run Off*, n.d.). A key case study from São Paulo found that a 24% substitution of conventional roofs with green roofs was sufficient to prevent canal overflow, a more efficient result than the 40% substitution required for permeable pavements to achieve the same effect (Samant, 2015). This highlights the remarkable capacity of green roofs as a "source control" measure.

### **3.2.1 Phase I: Model Parameterization**

This study is based on the drainage density layer which is one of layers used to develop flood risk map. The other layers used i.e., annual precipitation, elevation and distance to stream were not affected by green roof installation thus we will focus on the drainage density layer.

The vegetation on the roof doesn’t directly affect the drainage density of the area but it helps in reducing the hydrological load on the drainage system of the area. Green roofs are "source control" measures that intercept rainfall, increase infiltration, and extend the time it takes for water to enter the drainage system; they do not physically change the length of a stream or pipe (Dong et al., 2023). This reduces the rate of runoff as well as volume causing effective drainage of the water.

To model this, the Raster Calculator simplifies a complex hydrologic process by isolating prominent channels. It applies a threshold (Flow Accumulation > 1,000) which was (>10,000 in the case of Conventional roof) to extract main streams. This method enables a quick, city-wide assessment of green roof impact, eliminating the need for a dynamic hydrological process model.

### **3.2.2 Phase II: Creation of New Flood Map and Comparative Analysis**

The modified drainage density is then combined with the other layers using the same weighted overlay methodology used in the previous study. The new map shows the new flood risk map for the Montreal region in a scenario where all buildings are fitted with green roofs.

The final step and most critical step is to compare both the flood maps. The post-intervention flood map is subtracted from the baseline flood map to produce a final difference raster. The different areas show the changes seen in the flood risk hotspots due to the vegetation. A positive value indicates reduction in flood risk, while a zero or negative value indicates no change. This will help in quantitative assessment of flood mitigation benefit of green roof implementation.

### **3.3 Microclimate (UHI) Modelling**

#### **3.3.1 Tool Used in this study - ENVI-MET**

The efficacy of each UHI mitigation strategy will be evaluated through simulations conducted using ENVI-MET simulation software, which has already been used in the industry for a while (Ambrosini et al., 2014; Cortes et al., 2022; Iaria & Susca, 2022).

ENVI-MET is a three-dimensional non-hydrostatic microclimatic model that allows for complex modelling and detailed investigation of urban microclimate (O'Malley et al., 2015). ENVI-met simulates the temporal evolution of numerous thermodynamic parameters on a micro-scale scale, resulting in a 3D (2x2x2 grid cell in meters) non-hydrostatic model of the interactions between the building, atmosphere, and vegetation (Chatzinikolaou et al., 2018a). It can compute three-dimensional wind fields, turbulence, air temperature and humidity, radiative fluxes, and pollutant dispersion due to its physical foundations, which are based on the basic concepts of fluid mechanics, thermodynamics, and atmospheric physics (Bruse, 2004). The model's high spatial resolution, along with extensive vegetation modeling, enables simulation of individual photosynthetic rates while accounting for local solar radiation, air temperature and humidity, wind speed, CO<sub>2</sub> concentration, and a variety of other characteristics (Simon, n.d.).

ENVI-met software simulates firstly the microclimates' data and then estimates the selected thermal comfort index, through the Predicted Mean Vote (PMV) index (Chatzinikolaou et al., 2018b). PMV index evaluates the outdoor thermal comfort and summarizes the impact of the 4 main atmospheric variables: Air Temperature, Radiative Temperature, Wind Speed and Humidity on the human thermal sensation (Chatzinikolaou et al., 2018c).

Required data for ENVI-Met

The necessary input data for the ENVI-Met model include latitude and longitude, the simulation date and duration, the horizontal wind speed, cloud cover, the roughness length, the air temperature, and the specific and relative humidity (Bruse, n.d.).

The variables computed by ENVI-Met are:

- Wind speed and Direction
- Potential Air temperature
- Air and Soil Humidity
- Radiative Flux
- Gas particle dispersion
- Contour Lines

- Direct, Diffuse and Reflected Radiation
- CO2 (ppm)
- Specific and Relative humidity

### **3.3.2 Basic Model and Simulation with ENVI-Met:**

In ENVI-met, the simulation procedure typically simulates 24 to 48 hours. Initializing the model at night or at sunrise is the best way to guarantee that the simulation replicates atmospheric processes. ENVI-met typically requires a one-hour spin-up time (Crank et al., 2018a).

### **3.3.3 Why is ENVI-Met used for this study?**

ENVI-met is widely used in outdoor microclimate simulations due to its reliability in modeling thermal performance in urban environments. Its application in various studies has demonstrated an acceptable agreement between measured field data and simulated results, making it a suitable tool for assessing urban climate conditions. Given the objectives of my study, ENVI-met is particularly valuable for evaluating the microclimatic effects of urban modifications, such as changes in surface materials, vegetation, and building configurations, on solar photovoltaic (PV) potential and overall energy performance.

Several studies have validated the accuracy and applicability of ENVI-met. (Lahme & Bruse, n.d.) demonstrated that ENVI-met could accurately reproduce observed weather conditions in a park in Essen, Germany, even without model calibration. (Yu & Hien, 2006) assessed the cooling impact of parks using ENVI-met, confirming its reliability in predicting urban temperature variations. (E. E. Aydin et al., n.d.) compared ENVI-met with other urban microclimate tools and concluded that its predictions fall within an acceptable error range while offering comprehensive simulation capabilities. Similarly, (*21st International Cartographic Conference 10-16 Augustus 2003 Icc, Durban. CD-Rom, 9999*) found that ENVI-met effectively modeled the impact of urban parks on microclimate conditions in Arizona, highlighting its potential for sustainable urban planning.

Despite its advantages, ENVI-met has certain limitations. (Crank et al., 2018b) and (Krayenhoff et al., 2021) noted that microscale models, including ENVI-met, do not fully account for local-scale advection or boundary-layer vertical mixing. (Ali-Toudert & Mayer, n.d.) pointed out that ENVI-met tends to overestimate nighttime temperatures due to the absence of regional exchange processes. Furthermore, (Tsoka et al., 2018) reviewed the accuracy of ENVI-met in simulating microclimate variables and found that while it tends to overestimate daytime mean radiant temperature, it remains reliable in capturing peak daytime values.

Nevertheless, ENVI-met remains the most comprehensive tool for analyzing outdoor comfort, given its ability to integrate multiple urban parameters. With a proper understanding of its limitations and accurate input data, it can effectively represent temperature indices in complex urban settings (Rosheidat & Bryan, 2010). This makes it an ideal choice for my study, where evaluating the microclimatic effects of urban surfaces on solar PV performance is crucial.

### 3.3.4 Flow Chart

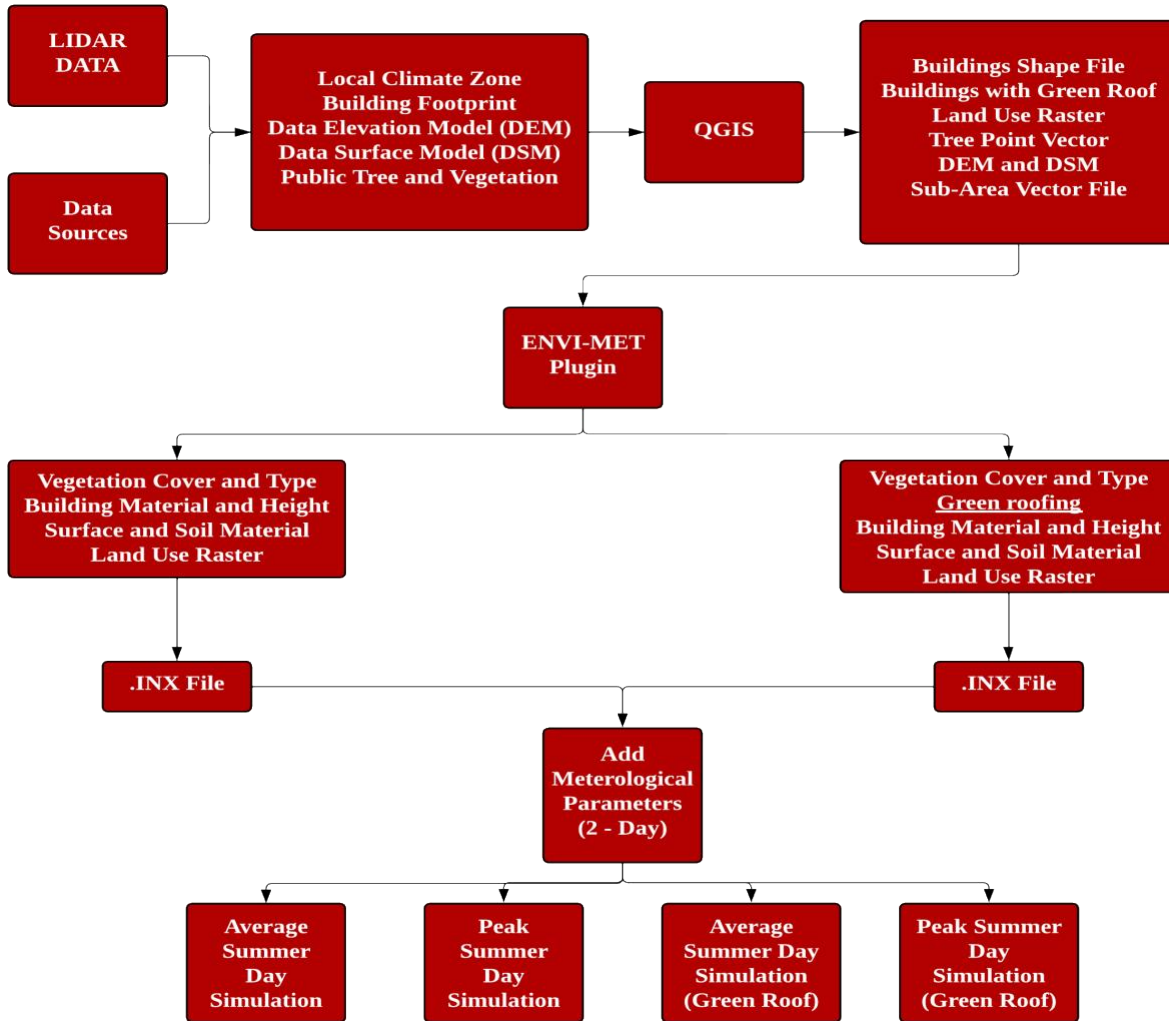


Figure 16. Methodology Flow Chart

### 3.3.5 Data Collection

The raw data for this study is acquired from multiple sources. Light Detection and Ranging (LiDAR) data, used for obtaining building footprints, is sourced from the Canadian Government’s open data portal. The Digital Elevation Model (DEM), Digital Surface Model (DSM), and vector data for public trees and vegetation are extracted from OpenStreetMap. Additionally, a land use raster file and the Local Climate Zone (LCZ) map are generated using Google Earth Engine (Demuzere et al., 2022).

### 3.3.6 Study Area Selection

The study focuses on areas within Montreal identified as high-temperature zones based on the Local Climate Zone classification.

### 3.3.7 Local Climate Zone

Stewart and Oke (Stewart & Oke, 2012b) established Local Climate Zones (LCZ) as a classification method for urban and rural environments based on land cover, land use, and built environment features. With unique thermal, physical, and aerodynamic characteristics, the LCZ system divides metropolitan regions into various zones, including industrial districts, open mid-rise, compact high-rise, and vegetated zones. The Urban Heat Island (UHI) effect, in which populated areas retain more heat than nearby rural areas, is frequently studied using this categorization.

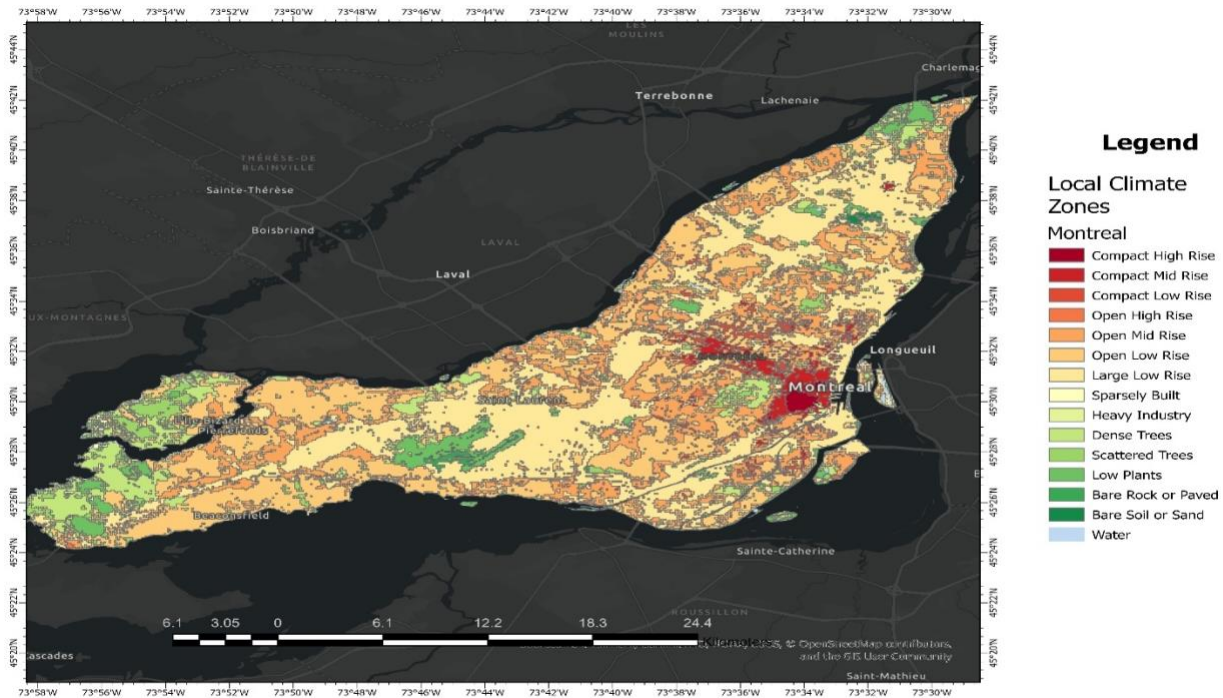


Figure 17. Local Climate Zones – Montreal Region

### 3.3.8 Study Area

Based on the LCZ, the area chosen to carry out this study is the Downtown region of Montreal, Canada. The study area consists of the total area of 327,405.6 m<sup>2</sup>. The study's focus is on highly populated urban areas with high UHI intensity, specifically downtown Montreal and the nearby business and residential areas, as determined by the LCZ analysis. Among the areas chosen are:

- High-rise structures, little greenery, and a lot of heat retention characterize the downtown core.
- Mixed urban areas with high heat accumulation are known as Compact Mid-rise zones.

This study aims to assess the cooling capability of green roofs and their efficacy in lowering urban heat stress in Montreal by combining LCZ categorization with field temperature measurements, satellite imaging, and urban planning factors.

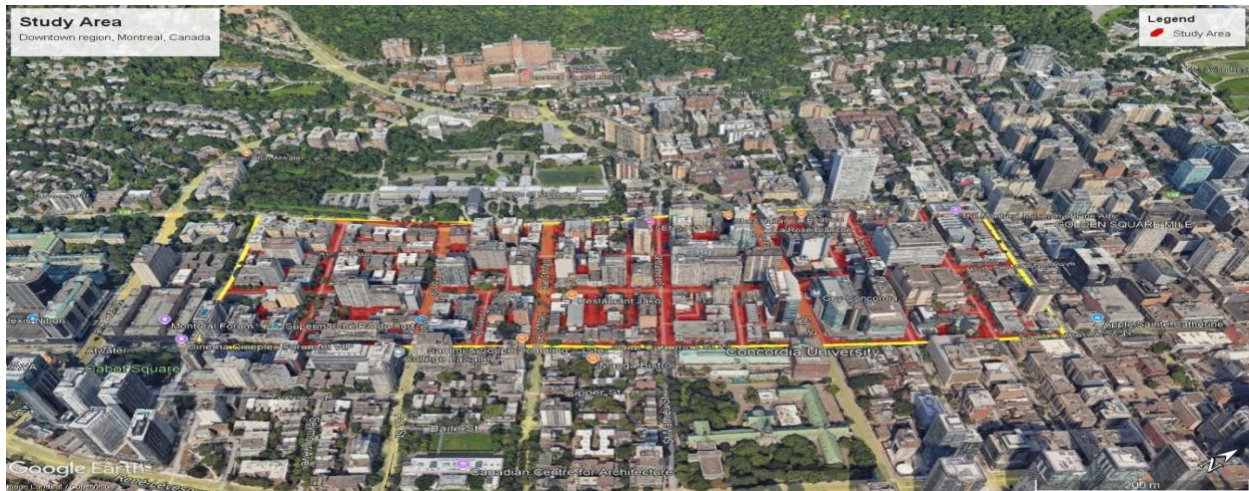


Figure 18. Study Area

### 3.3.9 Seasonality in Montreal – Case Study Specifics

Montreal typically experiences 4 seasons throughout the year. Mostly its Winter, spreading from December till March with temperatures ranging from  $-10^{\circ}\text{C}$  to  $-20^{\circ}\text{C}$  ( $14^{\circ}\text{F}$  to  $-4^{\circ}\text{F}$ ), though wind chills can make it feel even colder. Then, Spring comes which lasts till May with temperatures between  $10^{\circ}\text{C}$  to  $20^{\circ}\text{C}$  with frequent rainfall. Summer starts from June to August which feels warm and humid ( $0^{\circ}\text{C}$  to  $30^{\circ}\text{C}$ , sometimes exceeding  $35^{\circ}\text{C}$  with humidity). Autumn is cool and crisp with temperatures dropping from around  $15^{\circ}\text{C}$  in September to near freezing by November.

Over the years, the temperature of Montreal Island has increased by  $1.88^{\circ}\text{C}$  (McGill Weather station), which shows a significant increase in temperature (Bouchard & Qi, 2017). The Main reason is the increase of greenhouse gas emissions which further increases the atmospheric concentrations of carbon dioxide ( $\text{CO}_2$ ), methane ( $\text{CH}_4$ ) and nitrous oxide ( $\text{N}_2\text{O}$ ), resulting in extreme weather and climate events, as well as changes in temperature and precipitation (Calvin et al., 2023). The graph below shows the increase in average monthly temperature of the Montreal region over the year.

### 3.3.10 Data Preparation for ENVI-Met

Two separate building shapefiles are created: one representing buildings with green roofs and another with conventional roofs. These shapefiles include essential attributes such as building height, construction material, elevation, and exact building dimensions. Additional layers necessary for the ENVI-Met model are prepared, including:

- A public trees and vegetation layer with ENVI-Met-specific IDs.
- A land use raster file that classifies features according to ENVI-Met identifiers.
- A DEM file representing the topography of the Montreal region.

### 3.3.11 Simulation Details:

*Table 4. Simulation Detail*

<b>Simulation Input Data</b>	
Simulation Model Size (m)	370 x 358 x 28
Model Area (Number of grids)	50 x 50 x 36
Geographic Location (Latitude, Longitude)	45.5035° N, 73.5685° W
Method of Vertical grid generation	Equidistant
Reference time zone	GMT-5
<b>Main Model Parameters</b>	
Simulation date	19 <sup>th</sup> June 2024
Start and Duration of Simulation	18 <sup>th</sup> June 2024 ,18:00, 29 hours
Wind speed (m/s)	1.19 m/s
Wind Direction	160 degree
Max Temperature (°C)	33
Min Temperature (°C)	25
Max Humidity (%)	84
Min Humidity (%)	56
Specific Humidity at model top (2500m, g/kg)	8

*Table 5. Model Parameters*

<b>Main Model Parameters</b>	
Simulation date	5 <sup>th</sup> June 2024
Start and Duration of Simulation	4 <sup>th</sup> June 2024 ,18:00, 29 hours
Wind speed (m/s)	1.18 m/s
Wind Direction	160 degree
Max Temperature (°C)	29.1
Min Temperature (°C)	19.8
Max Humidity (%)	80

Min Humidity (%)	39
Specific Humidity at model top (2500m, g/kg)	8

Table 6. Material Detail

Element Type	Albedo
[C5] Concrete Wall (Cast Dense)	0.3
[GH] Medium Insulation Glass wall	0.2
[ST] Asphalt Road	0.2
[PP] Pavement (Concrete)	0.4
[LO] Loamy Road	0.0

Table 7. Tree Data

Tree Name	Envi MET ID
Acer x freemanii 'Autumn Fantasy'	30035
Amelanchier laevis	30035
Apple Serviceberry	020100
Ash	20080
Autumn Blaze Freeman Maple	10035
Basswood	000NNN
Bitternut Hickory	01AMDL
Black Locust	010MSL
Bur Oak	20440
Cathedral elm	30120
Columnar Norway Maple	30030
Common Honey-Locust	010MSL
Elm	30120
Emerald Queen Norway Maple	02003A
English Oak	20440
European Black Alder	20039
Fastigate English Oak	20040
Homestead Elm	20121
Kentucky Coffee Tree	20160
Maidenhair Tree	30150
Morton (Accolade TM) Elm	20121
Nom Anglais	30120
Norway Maple	30030
Skyline Honey-Locust	010MSL

ENVI-Met's plugin is integrated within QGIS, facilitating the export of all processed data to generate a .INX file. This file contains the spatial and environmental attributes required for simulation within ENVI-Met.

### 3.3.12 Weather Data of the Selected Days

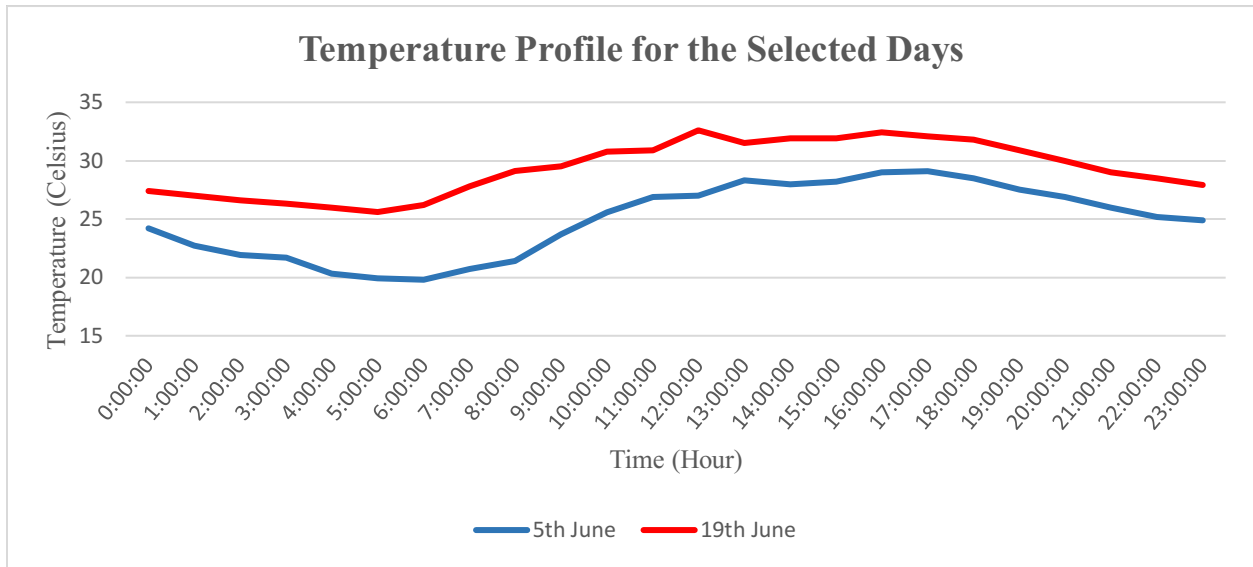
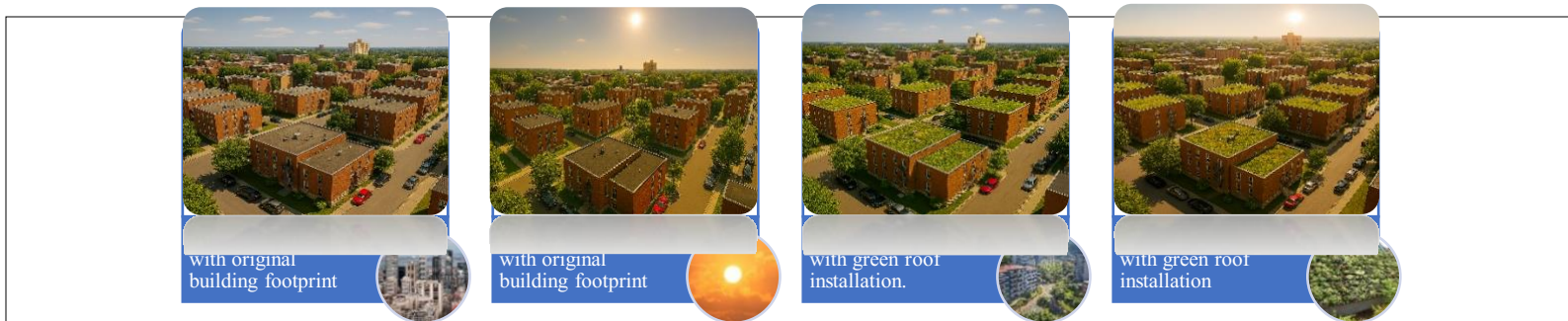


Figure 19. Weather Data

### 3.3.13 Simulations:



**\*Normal Condition – 5<sup>th</sup> June 2024**

**\*Peak Summer Day – 19<sup>th</sup> June 2024 (Max temp recoded is 39<sup>o</sup>C)**

The selected summer dates for analysis are June 5 and June 19, 2024. June 5 represents a typical summer day, chosen as a random reference point within the season. In contrast, June 19 was selected due to its record-high temperature of 39.0°C (Feel’s like due to high humidity), the highest recorded in Montreal during the summer of 2024.

1. **A peak summer day (June 19, 2024)**, representing extreme temperature conditions.
2. **A typical summer day**, reflecting average summer temperatures in Montreal.

A 30-hour weather dataset is integrated into the model, including:

- Six hours of data from the previous day for model training.
- Twenty-four hours of meteorological data for the simulation period.

The meteorological parameters used include air temperature, relative humidity, wind speed and direction, and cloud cover. Four distinct weather files are generated and incorporated into the model.

### 3.3.14 Study Area Model in Envi-MET

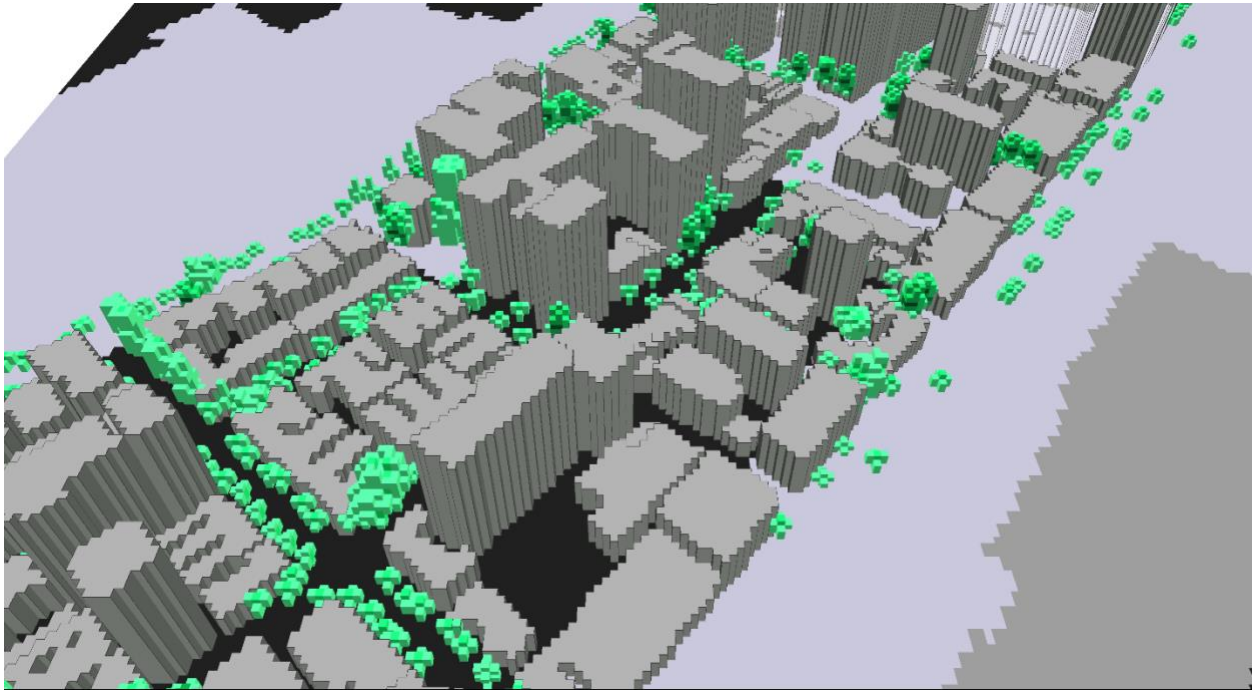
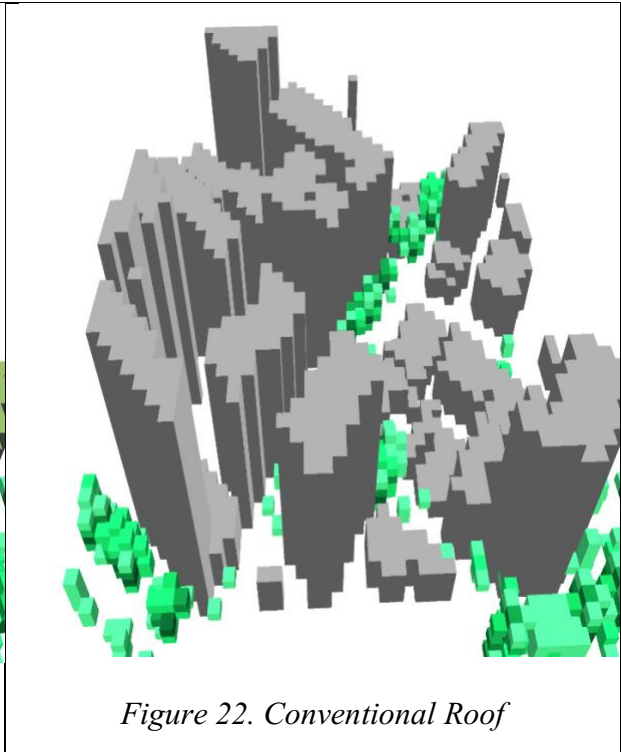
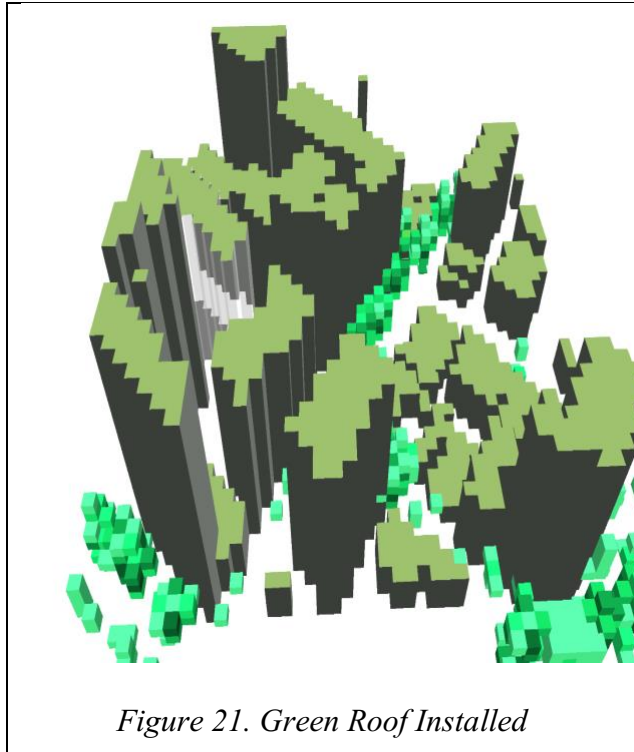


*Figure 20. Full Study Area Model*



### 3.3.15 Simulation File Generation

The combination of geometric and meteorological datasets results in the creation of **.SIMX** files, which serve as the simulation files for ENVI-Met. A total of four simulation files are generated for analysis.

*Table 8. Simulation Scenarios*

Scenerio-1	June-5 <sup>th</sup> 2024	General Summer Day	No Green Roof
Scenerio-2	June-19 <sup>th</sup> 2024	Peak Summer Day	No Green Roof
Scenerio-3	June-5 <sup>th</sup> 2024	General Summer Day	With Green Roof
Scenerio-4	June-19 <sup>th</sup> 2024	Peak Summer Day	With Green Roof

## Chapter 4 Result and Discussion

### 4.1 Effect of Increased Vegetation on Flood Risk Map of the Region

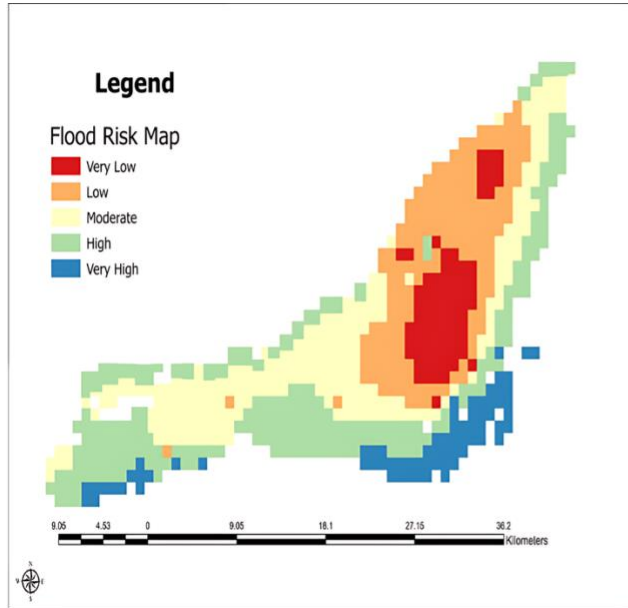


Figure 23. Original Flood Risk Map

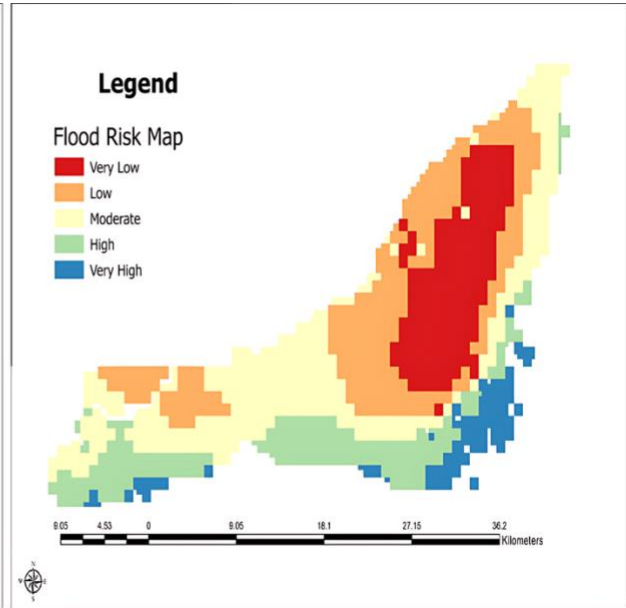


Figure 24. Modified Flood Risk Map

The figures depict the spatial variation of green roof impacts on flood risk, classified from very low (Negligible) to very high. High and very high impacts are concentrated in dense urban and flood-prone areas, where green roofs significantly reduce runoff and peak flows. Conversely, areas with less impervious cover display lower impacts due to limited additional hydrological benefits.

The study shows the reduction in flood prone area due to the installed green vegetation in the city. The extent and severity of flood-prone areas have clearly decreased, especially in the dense urban core where impervious surfaces are most common, according to the post-intervention map. Visually, the subtraction analysis yielded a raster that shows a decrease in flood risk across the whole study area, with the strongest effects seen in the highest-risk areas.

- The major drop in the flood risk is seen in the red, green zones representing dense urban area and coastal areas respectively due to the retention, delayed runoff and reduced peak flow which lowers effective drainage density.
- Some regions show no significant change, mainly because in those areas topographical and other factors dominate over the reduced run-off thus it shows less change.
- The flood risk reduction in areas with low building density indicates reduced runoff from green-roofed zones decreases downstream flood propagation. Flood risk reduction is driven by **hydrology and terrain**, not building density alone.

- Flood risk reduction is driven by hydrology and terrain, not building density alone, emphasizing the importance of watershed connectivity, elevation gradients and flow accumulation pathways in shaping the spatial extent of mitigation benefits.

Together, over 55% of the Montreal region (High + Very High Effect) experiences a significant reduction in flood risk due to the green roof installation. A "Moderate Effect" is apparent in 36.8% of the area, further indicating widespread positive hydrological effects. A small fraction of the area shows "Less Effect" (6.5%) or "Negligible Effect" (1.5%), which indicates widespread effectiveness across the urban area of green roofs.

## 4.2 Impact of Green Roofs on Urban Heat Island Mitigation

### 4.2.1 Simulation Design

Four simulation scenarios were developed using the ENVI-met microclimate modeling tool:

- **Simulation 1:**

*General Summer Day*

- Simulated at both maximum and minimum daily temperatures [without green roof installation](#).

- **Simulation 2:**

*Peak Summer Day*

- Simulated at both maximum and minimum daily temperatures [without green roof installation](#).

- **Simulation 3:**

*Peak Summer Day with Green Roof*

- Simulated at both maximum and minimum daily temperatures after [green roof installation](#).

- **Simulation 4:**

*General Summer Day with Green Roof*

- Simulated at both maximum and minimum daily temperatures after [green roof installation](#).

The Yellow highlighted text in the figures shows the elevation of the buildings.

#### 4.2.2 Comparative Analysis

To assess the thermal benefits of green roofs, temperature differentials were calculated between the no-green-roof and green-roof scenarios:

**Simulation 1 – Simulation 4: Average Summer Day – Maximum (17:00) and Minimum (6:00) temperature of the day**

#### Observations at Maximum temperature of the day

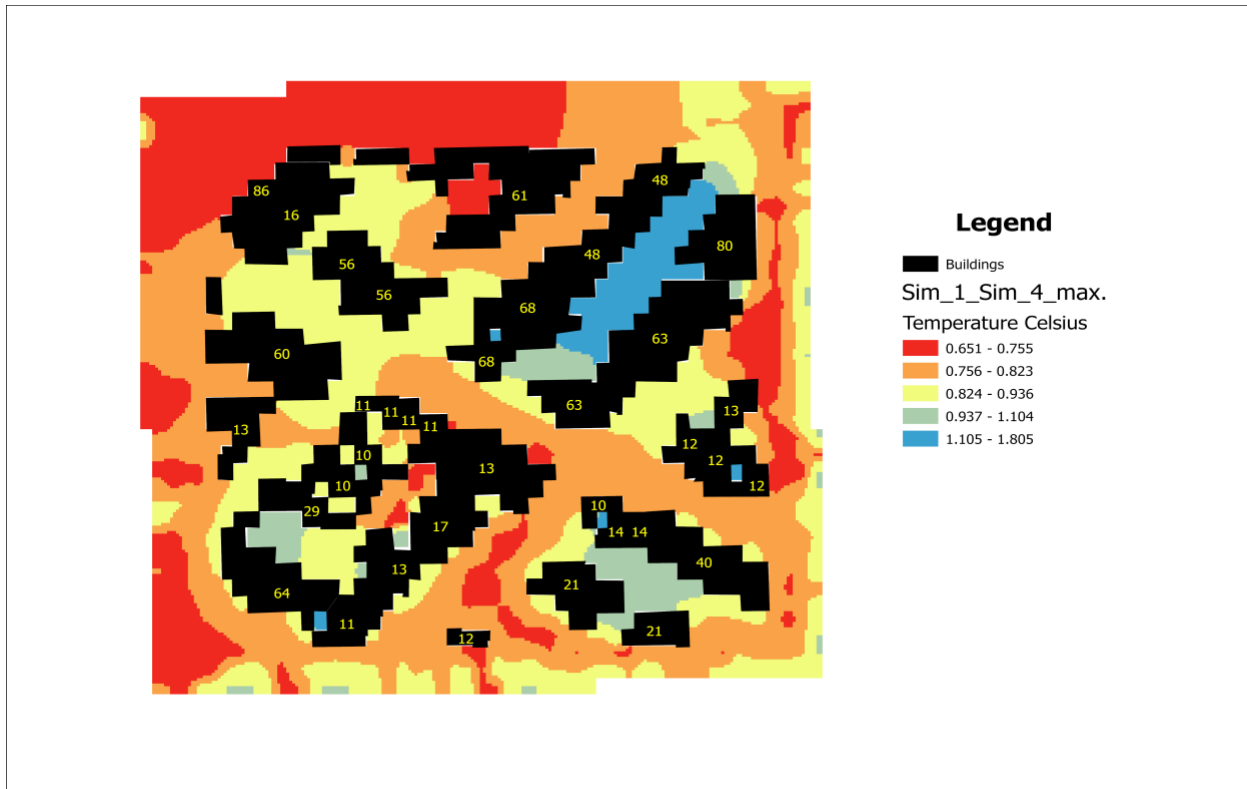
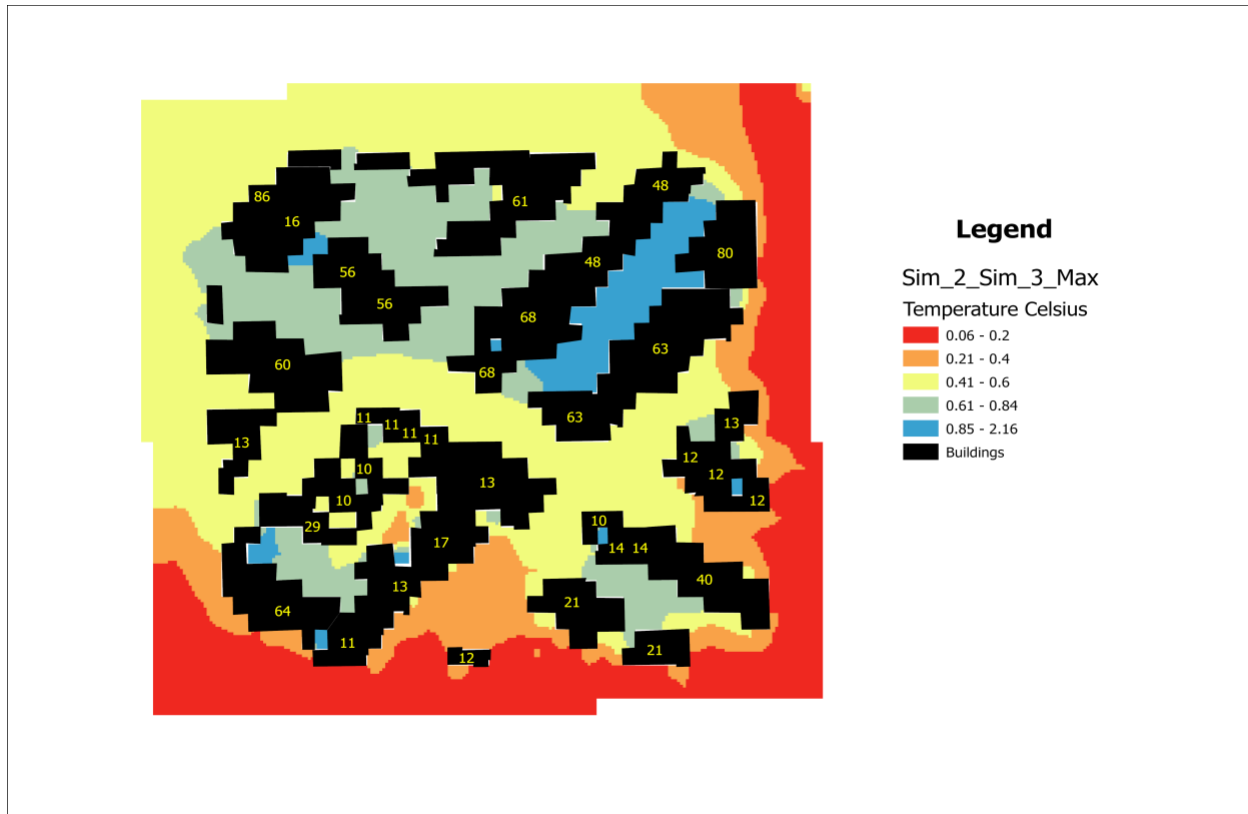


Figure 25: Temperature Difference on General Summer Day at Max Temperature

The highest temperature drops were observed near mid-rise buildings with full rooftop green coverage and dense urban zones, where UHI effects were most prominent pre-intervention.



*Figure 26: Temperature Difference on Peak Summer Day at Max Temperature*

The temperature reduction ranges from 0.06°C to 2.16°C, which is significant in an urban setting. It shows that green roof can provide a significant decrease in the pedestrian level temperature during a cruel summer day when the outside temperature is above 30<sup>0</sup> C.

The findings confirm the use of green infrastructure as a climate change adaptation strategy to enhance thermal comfort, public health, and energy efficiency in densely urbanized metropolitan cities like Montreal.

In both the cases, the observed temperature changes are due to the following reasons:

- **Maximum daytime cooling occurs within dense building clusters**, Areas adjacent to green roofs shows strong reduction due to evapotranspiration (sensible to latent heat)
- **Wind direction plays an important role**, in spatial spread and efficient downward mixing of cooler air over the green roofs through urban canyon airflow
- **Open and highly exposed spaces experience limited cooling**, as direct solar heating and warm pavement surfaces offset green-roof-induced temperature reductions
- **Shading as another dominant factor**, reduce shortwave radiation reaching the ground, reinforcing the cooling signal even where evapotranspiration is weaker

- **Higher temperature intensifies evapotranspiration, and air mixing, producing stronger but uneven cooling patterns (Shading dominates at the peak temperature)**

**Simulation 2 – Simulation 3:**

Temperature changes before and after green roof implementation on a peak summer day (both max and min temperatures).

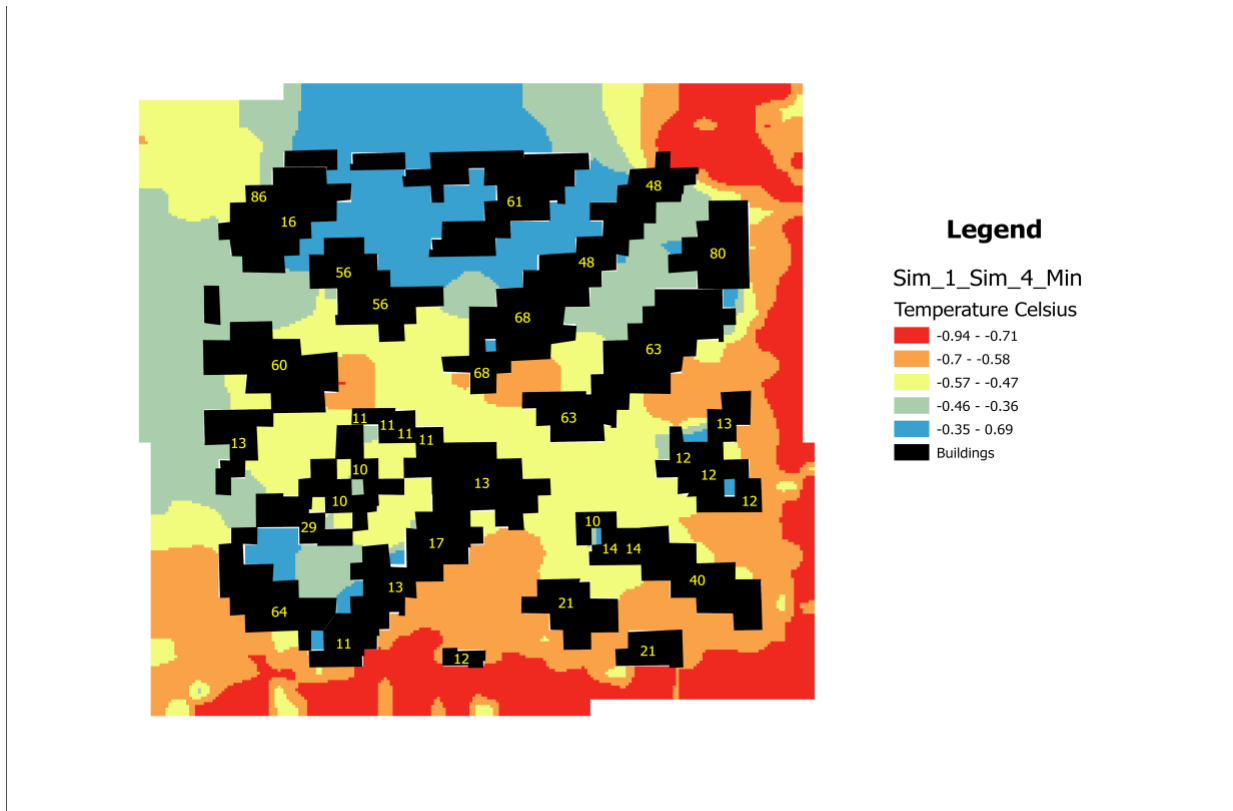


*Figure 27: Temperature Difference on General Summer Day at Min Temperature*

The green roof slightly reduces and, in some case, it actually increases the temperature at the pedestrian level during the minimum temperature of the observed day.

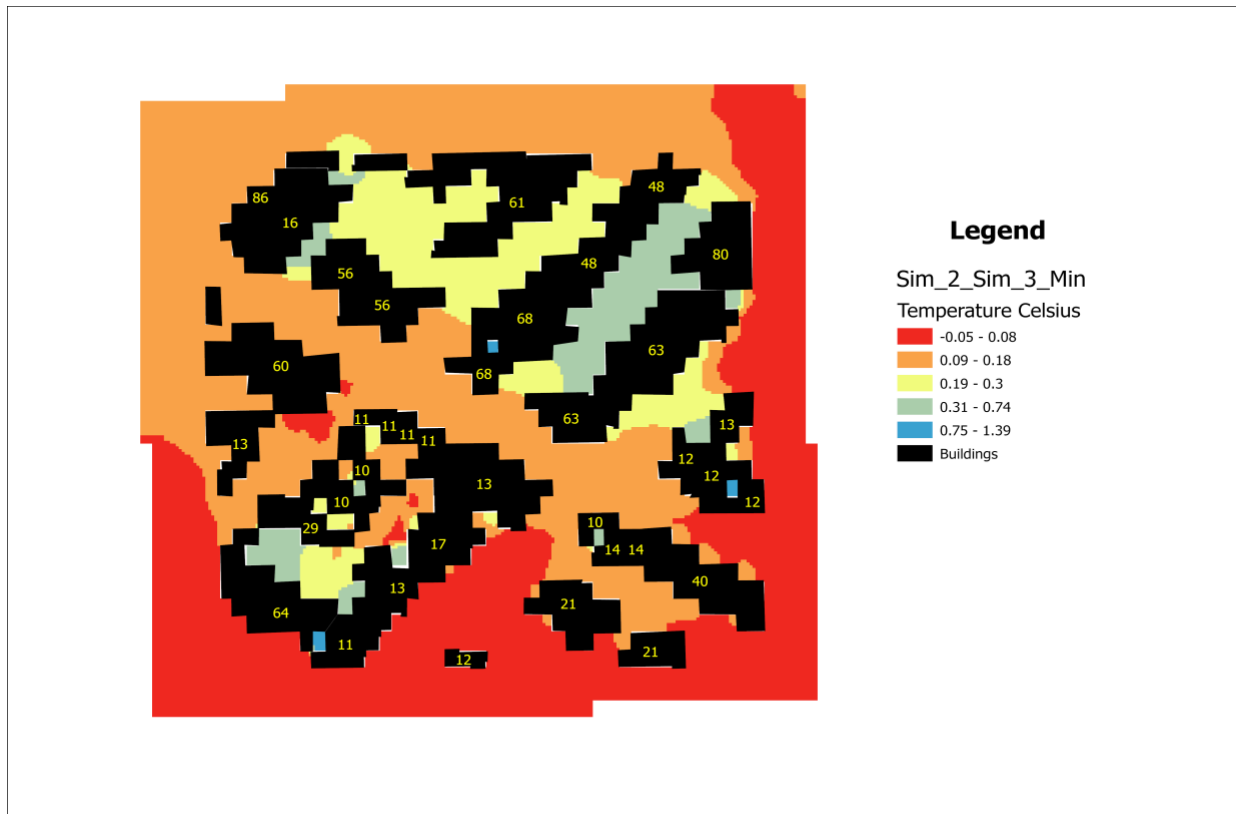


Figure 28: Temperature Difference on Peak Summer Day at Min Temperature

Majority of area shows decrease in temperature due to the green roofs. A few isolated areas showed slightly negative temperature differences, likely due to localized microclimatic interactions, model resolution effects, or delayed cooling behavior of green roof thermal mass.

Temperature variations were observed due to the following reasons:

- The main general observation is that the temperature increases at pedestrian level due to the green roofs.
- **“Warming Effect”** green roofs have high heat retention and slowly releases it during the nighttime. Conventional roofs radiate the heat quickly and cool quickly whereas the green roofs contain soil layer which retain moisture and during the daytime it absorbs solar radiation and at the nighttime it slowly releases it. Acting as high heat retention material.
- **Nighttime thermal response is governed by urban form rather than evapotranspiration**, reduced evapotranspiration at night.
- **“Canopy Effect”**, the greening act as a insulating layer over the soil which preventing it coming into direct contact with the cool night breeze and traps the heat inside.
- **Enclosed urban canyons, Open and peripheral zones experience** increased temperatures due to heat release from impervious surfaces, direct solar exposure, and warm

air accumulates in open space. In high elevation areas (>60 m) buildings form urban canyons where green roofs have the potential to confine evaporative cooling rather than disperse it horizontally. Convective heat dissipation may be impeded by stagnant air and decreased wind velocity. All these factors combine causes local temperature rise.

- **Orientation and Insolation**, In the afternoon, buildings that face southwest or south may experience high levels of solar insolation. If green roof has thin substrate layers and a dry substrate (less evapotranspiration), then it may act as a warm mass, absorbing heat rather than reducing it.

#### 4.2.3 Impact of Green Roofs on Pedestrian-Level Temperature during a Peak Summer Day

The graph shows the simulation where maximum reduction of temperature is observed i.e., Peak summer day at the time of maximum temperature of the day.

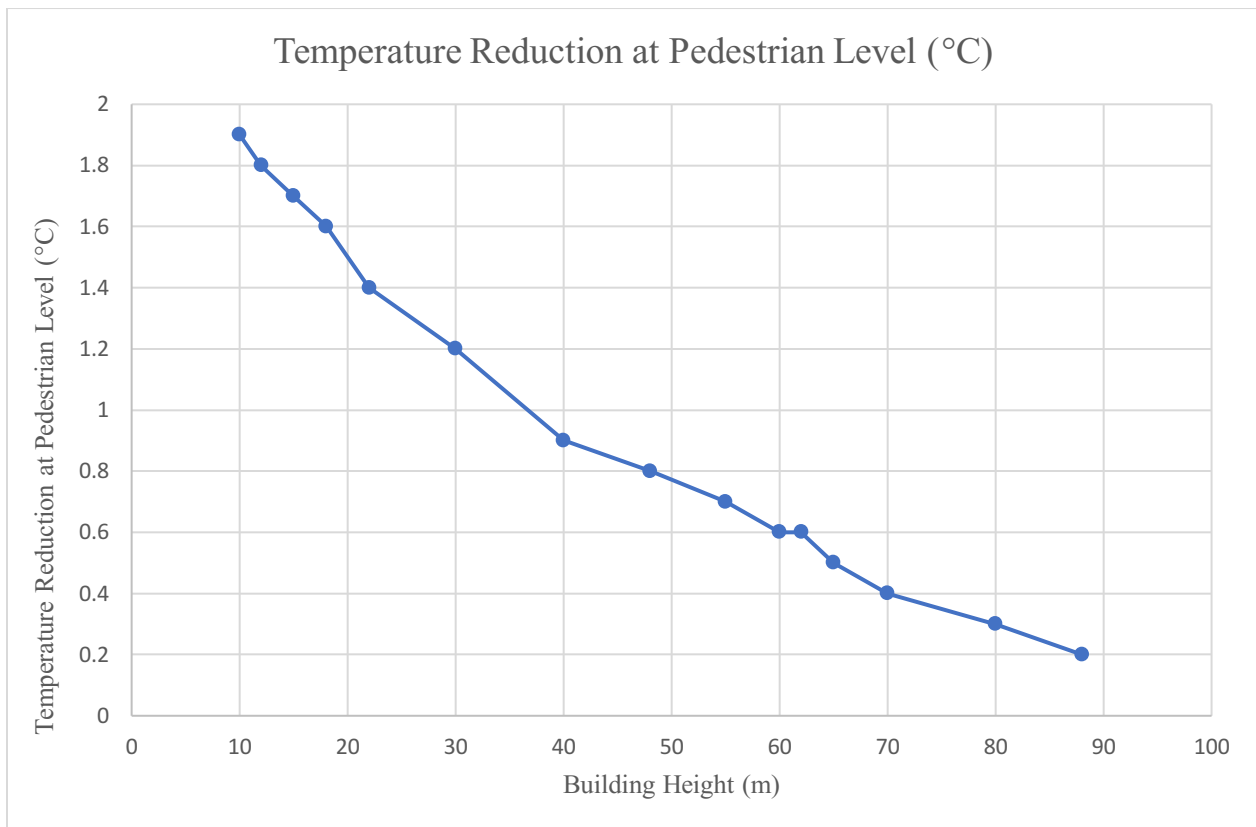


*Figure 29: Effect of building elevation on pedestrian level temperature*

The graph above clearly shows that as building height increases, the effect of green roof top on the pedestrian level decreases. This shows that the cooling effect from the vegetation is more directly

transferred to the ground level when the roof is closer to the pedestrian level. When the elevation increases, other factors come into major role for reducing the temperature at pedestrian level. Green roofs on low-rise buildings should be a top priority for city planners to get the most cooling benefits for people walking by.

#### 4.2.4 Comparison of 24-Hour Pedestrian-Level Air Temperature with and without Green Roofs

On a peak summer day, green roof can act very effectively which can be seen clearly in the graph below. The graph shows the temperature of a peak summer day with conventional roof vs the green roof.

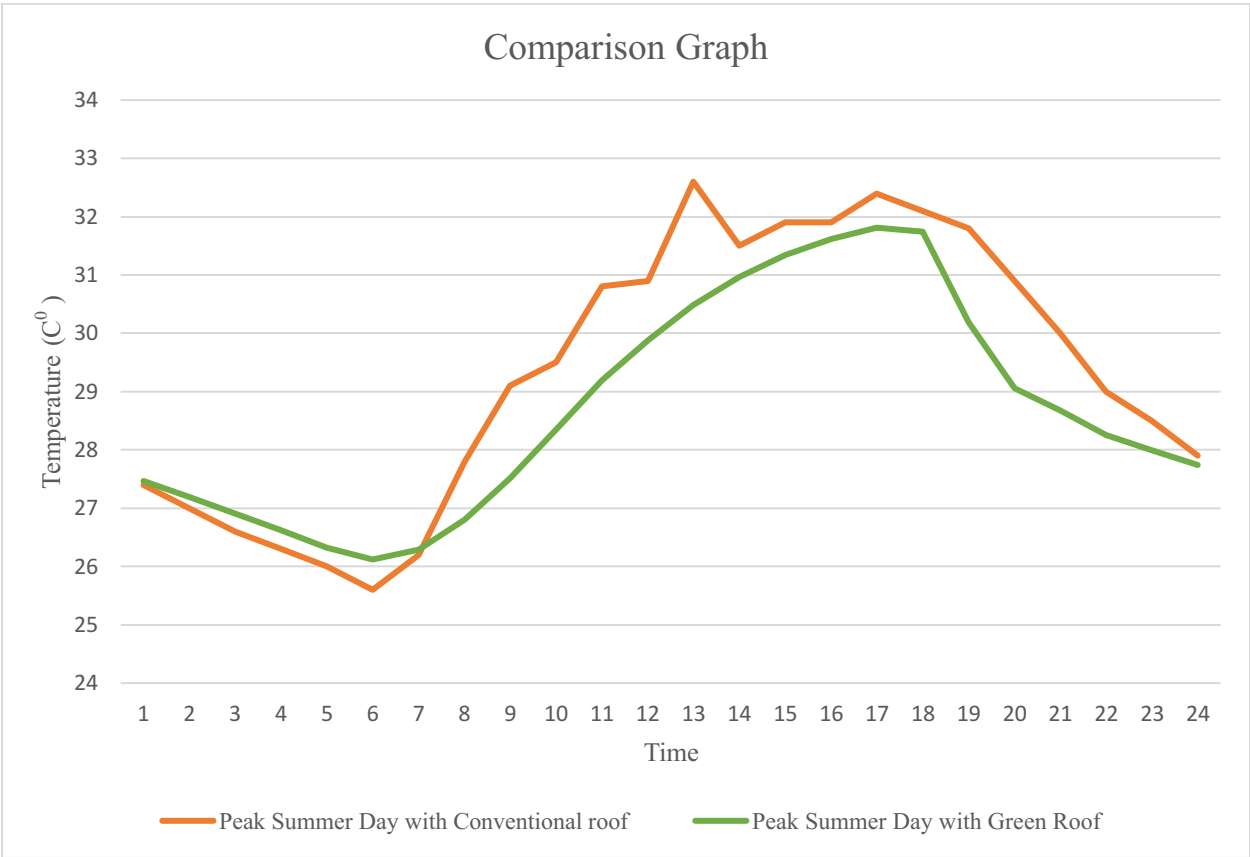


Figure 30: Peak Summer Day Temperature

The main observed scenarios from the graph shows that during the nighttime to early morning, the green roof is slightly warmer due to slow nighttime heat release from the vegetated roof layers.

As the sun comes up, temperatures rise faster for the conventional roof, as impervious surfaces absorb solar radiation efficiently, while green roofs delay heating through evapotranspiration and higher thermal inertia.

Midday to afternoon peak (Hours 12–17): The largest difference is observed here. The green roof consistently reduces area-averaged temperature ( $\approx 0.8\text{--}1.2$  °C lower) by converting sensible heat into latent heat and limiting heat storage whereas the conventional roof reaches the highest peak temperature, intensifying urban heat stress.

Evening cooling phase (Hours 18–24): Temperatures decline in both cases, but the green roof shows a faster cooling rate, indicating reduced daytime heat storage compared to conventional roofs.

The moderated temperature profile observed under the green roof scenario is due to the combined effects of evapotranspiration, shade, and lower heat storage within vegetated roof systems. Green roofs not only reduce daytime temperature peaks, but they also promote faster cooling in the evenings, minimizing nocturnal heat retention and limiting the persistence of urban heat islands. The reduced diurnal temperature amplitude supports the establishment of a more thermally stable microclimate, which is advantageous for pedestrian thermal comfort and urban livability.

### **4.3 Discussion of Synergistic Benefits**

This research provides a quantitative assessment of the dual effectiveness of green roofs, demonstrating how a single intervention addresses two of Montreal's most critical urban challenges: the Urban Heat Island (UHI) effect and flood risk. This study has significantly contributed to the microclimatic advantages of green roofs as well as to the potential of green roofs as a long-term, sustainable UHI mitigating strategy. At the same time, the research demonstrates that the widespread adoption of green roofs is a highly effective urban flood mitigating strategy. The mechanisms of both benefits are different yet complementary. For thermal control, the research verified that green roofs facilitate both direct and indirect cooling mechanisms such as reduced solar heat absorption, evapotranspiration, as well as thermal insulation. For hydrology, the green roof functions as a "source control" by minimizing the hydrological stress imposed by the city's drainage system, leading to easy draining away of the surplus waters creating the flood-like situation.

The results demonstrate the significance of green roofs in reducing extreme temperature events in urban settings by confirming that they have the strongest cooling effects during times of high heat. The observed decrease in flood-prone areas also aligns with existing research, which shows that green roofs can dramatically lower runoff volume and peak flow rates. This study lists several advantages of urban vegetation and shows how small-scale interventions can add up to major citywide benefits. In urban environments, the combination of lower temperatures and higher humidity improves thermal comfort and lessens the demand on energy-intensive cooling systems. The study therefore offers strong foundation for the policymakers and urban planners to implement green roof as a solution for both cooling effects as well as reducing high run-off damages. Adoption of nature-based solutions, such as green roofs, will be essential in promoting sustainable urban growth and improving the livability of metropolitan areas as cities continue to grow and confront the growing challenges of climate change.

## **Chapter 5 Conclusion, Limitations of the Study and Future Works**

### **5.1 Conclusion**

The study creates a coherent city-scale methodology that connects hydrological dynamics, urban form, and pedestrian-level thermal conditions in a single decision-support pipeline by combining high-resolution microclimate simulations in ENVI-MET with a GIS-based multi-criteria flood risk mapping framework using Analytic Hierarchy Process.

This thesis demonstrates that large-scale implementation of green roofs can simultaneously reduce pluvial flood susceptibility and mitigate urban heat, particularly in dense, high-rise urban cores, thereby reinforcing their value as a multi-functional nature-based solution for climate-resilient cities. A 24-hour evaluation reveals a distinctive pattern of slightly warmer conditions during night and early morning due to stored heat release, followed by delayed morning warming, pronounced midday–afternoon cooling, and faster evening temperature decline compared with conventional roofs. The thermal analysis demonstrates that green roofs consistently lower pedestrian-level air temperatures during the day, with the strongest cooling observed under peak summer conditions and within compact building clusters.

The results shows that pedestrian cooling is strongly influenced by the geometry of urban canyons and is inversely correlated with building height. The highest temperature reductions are seen in mid-rise, closely spaced buildings and shaded corridors, while the benefits are more restricted in open, highly insulated areas. The results shows that pedestrian cooling is strongly influenced by the geometry of urban canyons and is inversely correlated with building height. The highest temperature reductions are seen in mid-rise, closely spaced buildings and shaded corridors, while the benefits are more restricted in open, highly insulated areas.

The differentiated nighttime response emphasizes the significance of temporal dynamics and urban morphology in developing interventions that balance thermal comfort and energy performance throughout the entire diurnal cycle. On average summer days, green roofs may locally raise minimum temperatures while attenuating extreme minima during peak heat. Methodologically, LCZ-based site selection, directly quantifying green roof impacts at the pedestrian level across building heights, and combining a transparent, consistency-checked AHP weighting scheme with a scalable GIS workflow that can be applied to other data-scarce urban regions without relying on lengthy historical flood inventories, the thesis advances existing research methodologically. These contributions give urban planners, engineers, and policymakers a solid, spatially explicit body of evidence to support zoning and building code revisions, direct investments in stormwater and heat-adaptation infrastructure, prioritize the installation of green roofs in critical hotspots, and incorporate multi-hazard resilience considerations into municipal climate action plans.

## 5.2 Research Questions

### **Q) How does the installation of green roofs affect the Urban Heat Island (UHI) effect in the Montreal region?**

The green roof implementation shows significant effect on Urban Heat Island in Montreal, mainly through air temperature reductions at pedestrian-level, particularly under extreme heat conditions. Microclimate modeling applied in this case shows two important findings:

**Peak Heat Reduction:** On a peak summer day, implementation of green roofs has been known to lower air temperatures at the pedestrian level significantly, between a low of 0.85 °C to as high as a value of 2.16 °C in select locations. It achieves the cooling due to various mechanisms like evapotranspiration, which seizes latent heat from the ambient air, and higher albedo than that of typical roofing material.

**Impact of Building Elevation:** It is shown in the research that there is a clear negative relationship between the vertical height of buildings and the cooling effectiveness of green roofs at the pedestrian level. Cooling effects are highest in low-rise buildings and diminish as the building rises, since the heat benefits are transferred to the ground level more efficiently when the green surface has a lower altitude.

### **Q) What are the potential environmental benefits associated with large-scale green roof implementation in Montreal?**

The thesis is mainly focused on two key environmental benefits that accompany widespread green roof adoption, positioning it as a successful multi-dimensional strategy for building urban climate resilience.

**Urban Heat Island Mitigation:** The primary heat benefit lies in the significant reduction of external air temperatures, thus improving thermal comfort, reducing energy demands for cooling, and mitigating heat-related health hazards.

**Urban Flood Risk Reduction:** Hydrological analysis indicates that green roof implementation across the city has the potential to significantly lower the region's flood susceptibility. By acting as a "source control" measure, green roofs contain and slow stormwater runoffs, thereby increasing demands onto urban drain infrastructure.

In addition to these measurable advantages, the background study also discovers various identified advantages, such as the mitigation of noise, expansion of biodiversity, and enhanced longevity of roofing membranes in being protected from ultraviolet rays and heat variations.

### **Q) How much can the installation of green roofs change runoff coefficients and hence lower the risk of urban flooding in the Montreal region?**

Green roof installation has the potential to significantly reduce the likelihood of urban floods through efficient mitigation of the hydrological demand on the drainage infrastructure, a proxy measure for altered runoff behavior. The designed model varies its flow accumulation threshold

in the GIS inquiry to mimic the effects of large areas of rainwater retention. Quantitative findings are considerable:

- Combined, a green roof scenario has a region-wide outcome of allowing a cumulative 55.2% of the region of Montreal a "High" (47.8%) or "Very High" (7.4%) level of flood hazard mitigation.
- The positive effects are vast, as indicated by the fact that 92% of the whole region has a "Moderate," "High," or "Very High" decrease in susceptibility to flood.
- Compared to this, only 8% of the region displays a "Less" or "Negligible" impact, which bears testament to the extremely efficient character of green roofs as a form of urban flood mitigation.

**Q) How does urbanization affect the spatial distribution and intensity of flood risks, and how does the distribution of impervious surfaces contribute to these risks?**

Urbanization fundamentally transforms the spatial arrangement and increases the extent of the dangers of flooding, primarily due to the massive coverage of natural, permeable grounds with impermeable surfaces like asphalt and concrete. It increases the threat of floods in several ways:

- **Greater Runoff Volume and Velocity:** Impervious surfaces don't allow rainwater infiltration to the ground, thus there has been a growing volume of surface runoff that flows at a higher velocity.
- **Overwhelmed Drainage Systems:** This increased runoff abbreviates hydrological response times and raises peak discharge velocities throughout storms, overwhelming the capacity of conventional urban drainage infrastructure and causing more frequent and severe flood occurrences.
- **Spatially Focused Risk:** The work highlights that spatial arrangement of imperviousness is crucial; compact urbanization can inherently bring about higher concentrations of flash floods than diffused urbanization, supporting the value of spatial planning as a key factor in risk mitigation.

**Q) What are the spatial links and synergies between urban heat islands and flood risk in Montreal, and how can GIS-based spatial studies help with climate-resilient urban planning?**

This thesis demonstrates that there are strong spatial synergies between Flood Risk and UHI, as both are driven by the same factor: high human-built density and low vegetation cover. The key identified synergy is that a single nature-based solution, green roofs, can address both individual climate hazards concurrently, and as a consequence, it is a highly cost-effective resilience-building strategy.

GIS-oriented spatial research is introduced as the key instrument for gaining these insights and supporting climate-resilient planning. Their dual function is:

- **Integrated Problem Definition:** GIS offers the forum to manage heterogeneous spatial data and, when coupled with a formal approach such as the Analytic Hierarchy Process (AHP),

makes possible a fact-supported, repeatable assessment of flood danger throughout a whole urban catchment.

- **Solution-Focused Scenario Examination:** Through the integration of the results derived from the GIS-driven flood model with microclimate simulations conducted using ENVI-MET, the research transcends mere risk mapping to assess the dual advantages associated with a particular green infrastructure intervention. This data-informed methodology equips urban planners with the geographically explicit understanding essential for the strategic deployment of green infrastructure in locations where its efficacy can be maximized.

### **Q) What practical recommendations can spatial analysis and microclimate simulations provide to urban planners and policymakers as they implement effective green infrastructure solutions for climate-resilient urban design?**

The data analyses in this thesis make several evidence-based, practical recommendations for Montreal urban planners and policymakers:

- **Emphasize the Adoption of Green Roofs on Low-Rise Structures:** The most distinct suggestion emerging from the microclimate analysis is to emphasize the adoption of green roofs on low- and mid-rise structures. The data unequivocally indicates that the cooling effect experienced at the pedestrian level diminishes considerably as building height increases, suggesting that installations on shorter structures offer the most immediate thermal comfort advantages to the populace.
- **Adopt green infrastructure as a holistic strategy:** policymakers must regard green roofs as more than a series of dispersed fixes but as a powerful, multivalence approach to making a city more climate resilient. Double benefits described in terms of heat mitigation and flood control suggest that investments in green infrastructure can accomplish a range of municipal goals at once and thus deliver a higher return than piecemeal interventions.
- **Utilize Integrated Modeling for Long-Term Planning:** Planners must adopt integrated modeling systems similar to the one developed in this thesis to identify "hotspots" where heat and flood hazards intersect. By making it easier to position green infrastructure in the most vulnerable areas, it makes strategic use of its climate resilience benefits.

### **5.3 Limitations of the Study**

While this study has provided valuable insights into the impact of green roofs on mitigating the Urban Heat Island (UHI) effect and flood risk in Montreal, several limitations must be acknowledged:

- **Restricted Software Features (ENVI-MET Free Version)**

This study utilized the free version of ENVI-MET, which comes with limited computational capacity, restricting the complexity and scale of simulations. Advanced features such as higher-resolution modeling, extended simulation times, and detailed vegetation interactions were not fully available, potentially impacting result accuracy.

- **Limited Building Data Availability**

The study relied on freely available building data, which may not have included detailed architectural elements, thermal properties, and material-specific characteristics. The lack of precise building height and facade details might have influenced the accuracy of heat transfer and shading effects in the simulation.

- **Absence of High-Quality Digital Elevation Model (DEM) and Digital Surface Model (DSM)**

This constraint may have affected the accuracy of wind flow modeling, surface heat interactions, and terrain-based temperature variations in the simulations.

- **Lack of Long-Term Observational Data and no precipitation conditions observed**

The study primarily relied on short-term simulation outputs, without real-world long-term observational validation under different seasonal and climatic conditions. The simulation no precipitation data which affects the observed temperature data during the observed.

- **Assumption Scenario**

The model considers city wide green roof implementation which is not achievable as many buildings are constructed long back and building green roof on top it them can cause structural damage to the building. And sometimes it is practically not possible to construct green roof on the buildings because of the shape and size of the roof.

- **Simplified Hydrological Modeling**

The flow accumulation is taken as ( $>1000$ ) which is consider only main streams going down the drain and absorbed by the land. The model ignores the spatial distribution of rainfall intensity, soil conditions that came before the rainfall, or any of the design types of green roofs (e.g. extensive versus intensive) that can profoundly impact the retention capacity of water. For instance, this model ignores that a saturated green roof has a diminished capacity to accept additional rainfall. It does not include the complex physical processes like evaporation, transpiration which will affect the hydrological model.

Despite these limitations, the study provides a strong foundation for future UHI mitigation strategies and highlights the potential of green roofs in improving urban thermal environments. Future studies can address these constraints by leveraging advanced software versions, high-resolution geographic datasets, and real-world energy monitoring systems to enhance result accuracy and applicability.

## **5.4 Future Work**

While this study has demonstrated the effectiveness of green roofs in mitigating the Urban Heat Island (UHI) effect in Montreal, additional strategies can be explored to further enhance cooling

benefits and improve urban microclimates. As well as the flood risk mapping can also be improved by the following strategies.

To build on this research, future work can focus on the following aspects:

- **Incorporation of Roadside Vegetation and Urban Forestry**

Investigate the impact of tree canopy coverage along major streets in reducing surface and ambient temperatures. Conduct simulations to compare the cooling potential of green roofs versus roadside vegetation or a combination of both. Assess the role of tree species selection, leaf density, and seasonal variations in optimizing cooling efficiency.

- **Long-Term Performance and Precipitation Data**

Conduct multi-year simulations to understand the long-term impact of green roofs on temperature and humidity regulation. Adding precipitation data as well to investigate the effect of precipitation on the temperature readings.

- **Smart Urban Climate Modeling**

Utilize advanced technologies such as IoT-based climate sensors and AI-driven data analysis to monitor real-time temperature and humidity variations in green infrastructure projects. Develop GIS-based predictive models to identify the most effective locations for implementing green roofs and roadside vegetation.

- **Expansion of Research to Other Climatic Regions**

Conduct similar studies in different climatic zones, including arid, tropical, and temperate cities, to evaluate the effectiveness of green infrastructure in diverse environmental conditions. Compare results with existing UHI mitigation strategies in cities worldwide to derive globally applicable solutions.

- **Energy analysis**

Quantifying the difference in total energy consumption in buildings with and without green roofs. By reducing surface temperatures and improving insulation, green roofs have the potential to lower cooling energy demands during summer and reduce heating energy loss in winter.

- **Advanced Hydrological Modelling**

Instead of a simplified GIS proxy, future work could integrate dynamic hydrological models (like SWMM) to simulate rainfall-runoff processes more accurately. This would allow for a more precise quantification of how green roofs reduce peak flow rates and runoff volumes under different storm conditions.

By expanding the scope of this study to include roadside vegetation and hybrid cooling solutions, we can develop a more comprehensive and sustainable approach to UHI mitigation (Islam, 2024). These future research directions will help urban planners and policymakers make data-driven decisions for designing climate-resilient and livable cities.

## Bibliography

1. *21st International Cartographic Conference 10-16 Augustus 2003 Icc, Durban. CD-Rom.* (9999).
2. Abedini, M., Abedini, M., Tulabi, S., & Tulabi, S. (2018). Assessing LNRF, FR, and AHP models in landslide susceptibility mapping index: a comparative study of Nojian watershed in Lorestan province, Iran. *Environmental Earth Sciences*. <https://doi.org/10.1007/s12665-018-7524-1>
3. Agonafir, C., Lakhankar, T., Khanbilvardi, R., Krakauer, N., Radell, D., & Devineni, N. (2023a). A review of recent advances in urban flood research. In *Water Security* (Vol. 19). Elsevier B.V. <https://doi.org/10.1016/j.wasec.2023.100141>
4. Agonafir, C., Lakhankar, T., Khanbilvardi, R., Krakauer, N., Radell, D., & Devineni, N. (2023b). A review of recent advances in urban flood research. *Water Security*, 19, 100141. <https://doi.org/10.1016/j.wasec.2023.100141>
5. Ali-Toudert, F., & Mayer, -Helmut. (n.d.). *EFFECTS OF STREET DESIGN ON OUTDOOR THERMAL COMFORT*.
6. Al-Obaidi, K. M., Ismail, M., & Abdul Rahman, A. M. (2014). Passive cooling techniques through reflective and radiative roofs in tropical houses in Southeast Asia: A literature review. *Frontiers of Architectural Research*, 3(3), 283–297. <https://doi.org/10.1016/j.foar.2014.06.002>
7. Ambrosini, D., Galli, G., Mancini, B., Nardi, I., & Sfarra, S. (2014). Evaluating Mitigation Effects of Urban Heat Islands in a Historical Small Center with the ENVI-Met® Climate Model. *Sustainability*, 6(10), 7013–7029. <https://doi.org/10.3390/su6107013>
8. Ameri, A. A., Ameri, A. A., Keesstra, S., Pourghasemi, H. R., Pourghasemi, H. R., Cerdà, A., & Cerdà, A. (2018). Erodibility prioritization of sub-watersheds using morphometric parameters analysis and its mapping: A comparison among TOPSIS, VIKOR, SAW, and CF multi-criteria decision making models. *Science of The Total Environment*. <https://doi.org/10.1016/j.scitotenv.2017.09.210>
9. Angel, S., Sheppard, S. C., With, D. L. C., Buckley, R., Chabaeva, A., Gitlin, L., Kraley, A., Parent, J., & Perlin, M. (2005). *The Dynamics of Global Urban Expansion*. <http://www.williams.edu/Economics/UrbanGrowth/DataEntry.htm>.
10. Aydin, E. E., Jakubiec, J. A., & Jusuf, S. K. (n.d.). *A Comparison Study Of Simulation-Based Prediction Tools For Air Temperature And Outdoor Thermal Comfort In A Tropical Climate*. 4118–4125. <https://doi.org/10.26868/25222708.2019.210296>

11. Aydin, M. C., & Sevgi Birincioglu, E. (2022). Flood risk analysis using gis-based analytical hierarchy process: a case study of Bitlis Province. *Applied Water Science*, 12(6). <https://doi.org/10.1007/s13201-022-01655-x>
12. Bechtel, B., Demuzere, M., & Stewart, I. D. (2020). A Weighted Accuracy Measure for Land Cover Mapping: Comment on Johnson et al. Local Climate Zone (LCZ) Map Accuracy Assessments Should Account for Land Cover Physical Characteristics that Affect the Local Thermal Environment. *Remote Sens.* 2019, 11, 2420. *Remote Sensing*, 12(11), 1769. <https://doi.org/10.3390/rs12111769>
13. BELHADJ, B. K. FIRAS. (2020a). *MATHEMATIQUES*. EDITIONS UNIVERSITAIRES E.
14. BELHADJ, B. K. FIRAS. (2020b). *MATHEMATIQUES*. EDITIONS UNIVERSITAIRES E.
15. Bouchard, E., & Qi, Z. (2017). Long-term trends of climate change and its impact on crop growing season on Montreal Island. *Journal of Water and Climate Change*, 8(1), 78–88. <https://doi.org/10.2166/wcc.2016.139>
16. Bruse, M. (n.d.). *Simulating microscale climate interactions in complex terrain with a high-resolution numerical model: A case study for the Sydney CBD Area (Model Description)*.
17. Bruse, M. (2004). *ENVI-met 3.0: Updated Model Overview*. [www.envi-met.com](http://www.envi-met.com)
18. Büchele, B., Büchele, B., Kreibich, H., Kreibich, H., Kron, A., Kron, A., Thielen, A. H., Thielen, A. H., Ihringer, J., Ihringer, J., Oberle, P., Oberle, P., Merz, B., Merz, B., Nestmann, F., & Nestmann, F. (2006). Flood-risk mapping: contributions towards an enhanced assessment of extreme events and associated risks. *Natural Hazards and Earth System Sciences*. <https://doi.org/10.5194/nhess-6-485-2006>
19. Calheiros, C. S. C., & Stefanakis, A. I. (2021). Green Roofs Towards Circular and Resilient Cities. *Circular Economy and Sustainability*, 1(1), 395–411. <https://doi.org/10.1007/s43615-021-00033-0>
20. Calvin, K., Dasgupta, D., Krinner, G., Mukherji, A., Thorne, P. W., Trisos, C., Romero, J., Aldunce, P., Barret, K., Blanco, G., Cheung, W. W. L., Connors, S. L., Denton, F., Diongue-Niang, A., Dodman, D., Garschagen, M., Geden, O., Hayward, B., Jones, C., ... Ha, M. (2023). *IPCC, 2023: Climate Change 2023: Synthesis Report, Summary for Policymakers. Contribution of Working Groups I, II and III to the Sixth Assessment Report of the Intergovernmental Panel on Climate Change [Core Writing Team, H. Lee and J. Romero (eds.)]. IPCC, Geneva, Switzerland.* (P. Arias, M. Bustamante, I. Elgizouli, G. Flato, M. Howden, C. Méndez-Vallejo, J. J. Pereira, R. Pichs-Madruga, S. K. Rose, Y. Saheb, R. Sánchez Rodríguez, D. Ürge-Vorsatz, C. Xiao, N. Yassaa, J. Romero, J. Kim, E. F. Haites, Y. Jung, R. Stavins, ... Y. Park, Eds.). <https://doi.org/10.59327/IPCC/AR6-9789291691647.001>
21. Chatzinikolaou, E., Chalkias, C., & Dimopoulou, E. (2018a). URBAN MICROCLIMATE IMPROVEMENT USING ENVI-MET CLIMATE MODEL. *The International Archives of the Photogrammetry, Remote Sensing and Spatial Information Sciences*, XLII–4, 69–76. <https://doi.org/10.5194/isprs-archives-XLII-4-69-2018>
22. Chatzinikolaou, E., Chalkias, C., & Dimopoulou, E. (2018b). Urban microclimate improvement using ENVI-MET climate model. *International Archives of the Photogrammetry, Remote Sensing and Spatial Information Sciences - ISPRS Archives*, 42(4), 69–76. <https://doi.org/10.5194/isprs-archives-XLII-4-69-2018>

23. Chatzinikolaou, E., Chalkias, C., & Dimopoulou, E. (2018c). URBAN MICROCLIMATE IMPROVEMENT USING ENVI-MET CLIMATE MODEL. *The International Archives of the Photogrammetry, Remote Sensing and Spatial Information Sciences*, XLII-4, 69–76. <https://doi.org/10.5194/isprs-archives-XLII-4-69-2018>
24. Cortes, A., Rejuso, A. J., Santos, J. A., & Blanco, A. (2022). Evaluating mitigation strategies for urban heat island in Mandaue City using ENVI-met. *Journal of Urban Management*, 11(1), 97–106. <https://doi.org/10.1016/j.jum.2022.01.002>
25. Costanzo, V., Evola, G., & Marletta, L. (2016). Energy savings in buildings or UHI mitigation? Comparison between green roofs and cool roofs. *Energy and Buildings*, 114, 247–255. <https://doi.org/10.1016/j.enbuild.2015.04.053>
26. Crank, P. J., Sailor, D. J., Ban-Weiss, G., & Taleghani, M. (2018a). Evaluating the ENVI-met microscale model for suitability in analysis of targeted urban heat mitigation strategies. *Urban Climate*, 26, 188–197. <https://doi.org/10.1016/j.uclim.2018.09.002>
27. Crank, P. J., Sailor, D. J., Ban-Weiss, G., & Taleghani, M. (2018b). Evaluating the ENVI-met microscale model for suitability in analysis of targeted urban heat mitigation strategies. *Urban Climate*, 26, 188–197. <https://doi.org/10.1016/j.uclim.2018.09.002>
28. Demuzere, M., Kittner, J., Martilli, A., Mills, G., Moede, C., Stewart, I. D., Van Vliet, J., & Bechtel, B. (2022). A global map of local climate zones to support earth system modelling and urban-scale environmental science. *Earth System Science Data*, 14(8), 3835–3873. <https://doi.org/10.5194/ESSD-14-3835-2022>
29. Demuzere, M., Orru, K., Heidrich, O., Olazabal, E., Geneletti, D., Orru, H., Bhawe, A. G., Mittal, N., Feliu, E., & Faehnle, M. (2014). Mitigating and adapting to climate change: Multi-functional and multi-scale assessment of green urban infrastructure. *Journal of Environmental Management*, 146, 107–115. <https://doi.org/10.1016/j.jenvman.2014.07.025>
30. Dong, Z., Bain, D. J., Gray, K. A., Akcakaya, M., & Ng, C. (2023). Modeling the hydrological benefits of green roof systems: applications and future needs. *Environmental Science: Water Research & Technology*, 9(12), 3120–3135. <https://doi.org/10.1039/D3EW00149K>
31. Douglas, I., Anderson, P. M. L., Goode, D., Houck, M. C., Maddox, D., Nagendra, H., & Yok, T. P. (Eds.). (2020). *The Routledge Handbook of Urban Ecology*. Routledge. <https://doi.org/10.4324/9780429506758>
32. Dwivedi, A., & Mohan, B. K. (2018). Impact of green roof on micro climate to reduce Urban Heat Island. *Remote Sensing Applications: Society and Environment*, 10, 56–69. <https://doi.org/10.1016/j.rsase.2018.01.003>
33. *ENGINEERING HYDROLOGY Fourth Edition*. (n.d.).
34. Feng, B., Zhang, Y., & Bourke, R. (2021a). Urbanization impacts on flood risks based on urban growth data and coupled flood models. *Natural Hazards*, 106(1), 613–627. <https://doi.org/10.1007/s11069-020-04480-0>
35. Feng, B., Zhang, Y., & Bourke, R. (2021b). Urbanization impacts on flood risks based on urban growth data and coupled flood models. *Natural Hazards*, 106(1), 613–627. <https://doi.org/10.1007/s11069-020-04480-0>
36. Fernández, D. S., Fernández, D. S., Lutz, M. A., & Lutz, M. A. (2010). Urban flood hazard zoning in Tucumán Province, Argentina, using GIS and multicriteria decision analysis. *Engineering Geology*. <https://doi.org/10.1016/j.enggeo.2009.12.006>

37. Fuladlu, K., Riza, M., & İlkan, M. (2018). *THE EFFECT OF RAPID URBANIZATION ON THE PHYSICAL MODIFICATION OF URBAN AREA* (Vol. 183, Issue 1). [http://coolparramatta.com.au/about\\_us](http://coolparramatta.com.au/about_us)
38. *Green Roofs & Storm Water Run Off*. (n.d.). Retrieved October 27, 2025, from <https://livingroofs.org/storm-water-run-off/>
39. Hayes, A., Jandaghian, Z., Lacasse, M., Gaur, A., Lu, H., Laouadi, A., Ge, H., & Wang, L. (2022a). Nature-Based Solutions (NBSs) to Mitigate Urban Heat Island (UHI) Effects in Canadian Cities. *Buildings*, 12(7), 925. <https://doi.org/10.3390/buildings12070925>
40. Hayes, A., Jandaghian, Z., Lacasse, M., Gaur, A., Lu, H., Laouadi, A., Ge, H., & Wang, L. (2022b). Nature-Based Solutions (NBSs) to Mitigate Urban Heat Island (UHI) Effects in Canadian Cities. *Buildings*, 12(7), 925. <https://doi.org/10.3390/buildings12070925>
41. Heaviside, C., Macintyre, H., & Vardoulakis, S. (2017). The Urban Heat Island: Implications for Health in a Changing Environment. *Current Environmental Health Reports*, 4(3), 296–305. <https://doi.org/10.1007/s40572-017-0150-3>
42. Huang, Q., Wang, J., Li, M., Fei, M., & Dong, J. (2017). Modeling the influence of urbanization on urban pluvial flooding: a scenario-based case study in Shanghai, China. *Natural Hazards*, 87(2), 1035–1055. <https://doi.org/10.1007/s11069-017-2808-4>
43. Iaria, J., & Susca, T. (2022). Analytic Hierarchy Processes (AHP) evaluation of green roof- and green wall- based UHI mitigation strategies via ENVI-met simulations. *Urban Climate*, 46, 101293. <https://doi.org/10.1016/j.uclim.2022.101293>
44. Islam, D. (2024). *A DECISION-RULE AND SPATIAL TRANSFER LEARNING-BASED APPROACH FOR AUTOMATED MAPPING OF LOCAL CLIMATE ZONES (LCZS) USING MULTI-SOURCE GEOSPATIAL AND REMOTE SENSING DATA* by.
45. Jamei, E., Chau, H. W., Seyedmahmoudian, M., & Stojcevski, A. (2021). Review on the cooling potential of green roofs in different climates. *Science of The Total Environment*, 791, 148407. <https://doi.org/10.1016/j.scitotenv.2021.148407>
46. Kachholz, F., Schilling, J., & Tränckner, J. (2021). A Model-Based Tool for Assessing the Impact of Land Use Change Scenarios on Flood Risk in Small-Scale River Systems—Part 2: Scenario-Based Flood Characteristics for the Planned State of Land Use. *Hydrology*, 8(3), 130. <https://doi.org/10.3390/hydrology8030130>
47. Kantiranis, N., Kantiranis, N., Kazakis, N., Kougias, I., Kougias, I., Patsialis, T., & Patsialis, T. (2015). Assessment of flood hazard areas at a regional scale using an index-based approach and Analytical Hierarchy Process: Application in Rhodope–Evros region, Greece. *Science of The Total Environment*. <https://doi.org/10.1016/j.scitotenv.2015.08.055>
48. Khosravi, K., Khosravi, K., Nohani, E., Nohani, E., Edris, M., Maroufinia, E., Keesstra, S., Pourghasemi, H. R., & Pourghasemi, H. R. (2016). A GIS-based flood susceptibility assessment and its mapping in Iran: a comparison between frequency ratio and weights-of-evidence bivariate statistical models with multi-criteria decision-making technique. *Natural Hazards*. <https://doi.org/10.1007/s11069-016-2357-2>
49. Khosravi, K., Khosravi, K., Shahabi, H., Shahabi, H., Pham, B. T., Pham, B. T., Adamowski, J., Adamowski, J., Shirzadi, A., Shirzadi, A., Pradhan, B., Pradhan, B., Dou, J., Dou, J., Ly, H., Ly, H.-B., Gróf, G., Gróf, G., Loc, H. H., ... Prakash, I. (2019). A comparative assessment

- of flood susceptibility modeling using Multi-Criteria Decision-Making Analysis and Machine Learning Methods. *Journal of Hydrology*. <https://doi.org/10.1016/j.jhydrol.2019.03.073>
50. Kim, J., Yeom, S., & Hong, T. (2025). Analyzing the cooling effect, thermal comfort, and energy consumption of integrated arrangement of high-rise buildings and green spaces on urban heat island. *Sustainable Cities and Society*, *119*, 106105. <https://doi.org/10.1016/j.scs.2024.106105>
51. Krayenhoff, E. S., Broadbent, A. M., Zhao, L., Georgescu, M., Middel, A., Voogt, J. A., Martilli, A., Sailor, D. J., & Erell, E. (2021). Cooling hot cities: a systematic and critical review of the numerical modelling literature. *Environmental Research Letters*, *16*(5), 053007. <https://doi.org/10.1088/1748-9326/abdcf1>
52. Kumar, N., & Jha, R. (2023). GIS-based Flood Risk Mapping: The Case Study of Kosi River Basin, Bihar, India. In *Technology & Applied Science Research* (Vol. 13, Issue 1). [www.etasr.com](http://www.etasr.com)
53. Lahme, E., & Bruse, M. (n.d.). *MICROCLIMATIC EFFECTS OF A SMALL URBAN PARK IN A DENSELY BUILD UP AREA: MEASUREMENTS AND MODEL SIMULATIONS*.
54. Landsberg, H. E. (1981). The urban climate. *International Geophysics Series*, *28*.
55. Liu, K. K. Y. ;, & Minor, J. (n.d.). *Performance evaluation of an extensive green roof*. [http://http://nparc.cisti-icist.nrc-cnrc.gc.ca/npsi/jsp/nparc\\_cp.jsp?lang=fr](http://http://nparc.cisti-icist.nrc-cnrc.gc.ca/npsi/jsp/nparc_cp.jsp?lang=fr)
56. Mokhtari, E., Mezali, F., Abdelkebir, B., & Engel, B. (2023). Flood risk assessment using analytical hierarchy process: A case study from the Cheliff-Ghrib watershed, Algeria. *Journal of Water and Climate Change*, *14*(3), 694–711. <https://doi.org/10.2166/wcc.2023.316>
57. Mosavi, A., Ozturk, P., & Chau, K. (2018). Flood Prediction Using Machine Learning Models: Literature Review. *Water*, *10*(11), 1536. <https://doi.org/10.3390/w10111536>
58. Moscrip, A. L., & Montgomery, D. R. (1997). URBANIZATION, FLOOD FREQUENCY, AND SALMON ABUNDANCE IN PUGET LOWLAND STREAMS <sup>1</sup>. *JAWRA Journal of the American Water Resources Association*, *33*(6), 1289–1297. <https://doi.org/10.1111/j.1752-1688.1997.tb03553.x>
59. Nsangou, D., Kpoumié, A., Mfonka, Z., Ngouh, A. N., Fossi, D. H., Jourdan, C., Mbele, H. Z., Mouncherou, O. F., Vandervaere, J. P., & Ndam Ngoupayou, J. R. (2022). Urban flood susceptibility modelling using AHP and GIS approach: case of the Mfoundi watershed at Yaoundé in the South-Cameroon plateau. *Scientific African*, *15*. <https://doi.org/10.1016/j.sciaf.2021.e01043>
60. Odli, Z. S. M., Zakarya, I. A., Mohd, F. N., Izhar, T. N. T., Ibrahim, N. M., & Mohamad, N. (2016). Green Roof Technology- Mitigate Urban Heat Island (UHI) Effect. *MATEC Web of Conferences*, *78*, 01100. <https://doi.org/10.1051/mateconf/20167801100>
61. Oke, T. R. (1982a). The energetic basis of the urban heat island. *Quarterly Journal of the Royal Meteorological Society*, *108*(455), 1–24. <https://doi.org/10.1002/qj.49710845502>
62. Oke, T. R. (1982b). The energetic basis of the urban heat island. *Quarterly Journal of the Royal Meteorological Society*, *108*(455), 1–24. <https://doi.org/10.1002/qj.49710845502>
63. O'Malley, C., Piroozfar, P., Farr, E. R. P., & Pomponi, F. (2015). Urban Heat Island (UHI) mitigating strategies: A case-based comparative analysis. *Sustainable Cities and Society*, *19*, 222–235. <https://doi.org/10.1016/j.scs.2015.05.009>

64. O'Malley, C., Piroozfarb, P. A. E., Farr, E. R. P., & Gates, J. (2014). An Investigation into Minimizing Urban Heat Island (UHI) Effects: A UK Perspective. *Energy Procedia*, 62, 72–80. <https://doi.org/10.1016/j.egypro.2014.12.368>
65. Papaioannou, G., Vasiliades, L., & Loukas, A. (2015). Multi-Criteria Analysis Framework for Potential Flood Prone Areas Mapping. *Water Resources Management*, 29(2), 399–418. <https://doi.org/10.1007/s11269-014-0817-6>
66. Pathirana, A., Deneke, H. B., Veerbeek, W., Zevenbergen, C., & Banda, A. T. (2014). Impact of urban growth-driven land use change on microclimate and extreme precipitation — A sensitivity study. *Atmospheric Research*, 138, 59–72. <https://doi.org/10.1016/j.atmosres.2013.10.005>
67. Rahman, M., Ningsheng, C., Mahmud, G. I., Islam, M. M., Pourghasemi, H. R., Ahmad, H., Habumugisha, J. M., Washakh, R. M. A., Alam, M., Liu, E., Han, Z., Ni, H., Shufeng, T., & Dewan, A. (2021). Flooding and its relationship with land cover change, population growth, and road density. *Geoscience Frontiers*, 12(6), 101224. <https://doi.org/10.1016/j.gsf.2021.101224>
68. Roberge, F., & Sushama, L. (2018). Urban heat island in current and future climates for the island of Montreal. *Sustainable Cities and Society*, 40, 501–512. <https://doi.org/10.1016/j.scs.2018.04.033>
69. Rosheidat, A., & Bryan, H. (2010). *OPTIMIZING THE EFFECT OF VEGETATION FOR PEDESTRIAN THERMAL COMFORT AND URBAN HEAT ISLAND MITIGATION IN A HOT ARID URBAN ENVIRONMENT*.
70. Roth, M., & Chow, W. T. L. (2012). A historical review and assessment of urban heat island research in Singapore. *Singapore Journal of Tropical Geography*, 33(3), 381–397. <https://doi.org/10.1111/sjtg.12003>
71. Samant, T. M. (2015). Green roofs pertaining to Storm Water Management in Urban Areas: Greening the City with Green Roofs. *IARJSET*, 2(10), 71–77. <https://doi.org/10.17148/IARJSET.2015.21015>
72. Samanta, S., & Koloa, C. (n.d.). Modelling Coastal Flood Hazard Using ArcGIS Spatial Analysis tools and Satellite Image. In *International Journal of Science and Research*. [www.ijsr.net](http://www.ijsr.net)
73. Shafique, M., Kim, R., & Rafiq, M. (2018). Green roof benefits, opportunities and challenges – A review. *Renewable and Sustainable Energy Reviews*, 90, 757–773. <https://doi.org/10.1016/j.rser.2018.04.006>
74. Simon, H. (n.d.). *Modeling urban microclimate*.
75. Speak, A. F., Rothwell, J. J., Lindley, S. J., & Smith, C. L. (2013). Rainwater runoff retention on an aged intensive green roof. *Science of The Total Environment*, 461–462, 28–38. <https://doi.org/10.1016/j.scitotenv.2013.04.085>
76. Stewart, I. D., & Oke, T. R. (2012a). Local Climate Zones for Urban Temperature Studies. *Bulletin of the American Meteorological Society*, 93(12), 1879–1900. <https://doi.org/10.1175/BAMS-D-11-00019.1>
77. Stewart, I. D., & Oke, T. R. (2012b). Local climate zones for urban temperature studies. *Bulletin of the American Meteorological Society*, 93(12), 1879–1900. <https://doi.org/10.1175/BAMS-D-11-00019.1>

78. Sun, X., Fang, P., Huang, S., Liang, Y., Zhang, J., & Wang, J. (2025). Impact of urban green space morphology and vegetation composition on seasonal land surface temperature: a case study of Beijing's urban core. *Urban Climate*, 60, 102367. <https://doi.org/10.1016/j.uclim.2025.102367>
79. Tang, Z., Tang, Z., Zhang, H., Zhang, H., Yi, S., Yi, S., Xiao, Y., & Xiao, Y. (2018). Assessment of flood susceptible areas using spatially explicit, probabilistic multi-criteria decision analysis. *Journal of Hydrology*. <https://doi.org/10.1016/j.jhydrol.2018.01.033>
80. Tehrany, M. S., Pradhan, B., & Jebur, M. N. (2014). Flood susceptibility mapping using a novel ensemble weights-of-evidence and support vector machine models in GIS. *Journal of Hydrology*, 512, 332–343. <https://doi.org/10.1016/j.jhydrol.2014.03.008>
81. Teng, J., Jakeman, A. J., Vaze, J., Croke, B. F. W., Dutta, D., & Kim, S. (2017). Flood inundation modelling: A review of methods, recent advances and uncertainty analysis. *Environmental Modelling & Software*, 90, 201–216. <https://doi.org/10.1016/j.envsoft.2017.01.006>
82. *The Analytic Hierarchy Process*. (n.d.).
83. Tsoka, S., Tsikaloudaki, A., & Theodosiou, T. (2018). Analyzing the ENVI-met microclimate model's performance and assessing cool materials and urban vegetation applications—A review. *Sustainable Cities and Society*, 43, 55–76. <https://doi.org/10.1016/j.scs.2018.08.009>
84. *URBAN HEAT ISLAND MITIGATION STRATEGIES: 2021 UPDATE NOVEMBER 2021 SYNTHESIS OF KNOWLEDGE*. (n.d.). <http://www.inspq.qc.ca/publications/2839>
85. *Vulnérabilité aux aléas climatiques de l'agglomération de Montréal*. (n.d.). Retrieved October 27, 2025, from <https://bter.maps.arcgis.com/apps/webappviewer/index.html?id=157cde446d8942d7b4367e2159942e05>
86. Wang, Y.-M., Liu, J., & Elhag, T. M. S. (2008). An integrated AHP–DEA methodology for bridge risk assessment. *Computers & Industrial Engineering*, 54(3), 513–525. <https://doi.org/10.1016/j.cie.2007.09.002>
87. Weng, Q. (2009). Thermal infrared remote sensing for urban climate and environmental studies: Methods, applications, and trends. *ISPRS Journal of Photogrammetry and Remote Sensing*, 64(4), 335–344. <https://doi.org/10.1016/j.isprsjprs.2009.03.007>
88. Wong, M. S., Nichol, J. E., To, P. H., & Wang, J. (2010). A simple method for designation of urban ventilation corridors and its application to urban heat island analysis. *Building and Environment*, 45(8), 1880–1889. <https://doi.org/10.1016/j.buildenv.2010.02.019>
89. Xu, F., & Gao, Z. (2022). Frontal area index: A review of calculation methods and application in the urban environment. *Building and Environment*, 224, 109588. <https://doi.org/10.1016/j.buildenv.2022.109588>
90. Yin, J., Yu, D., Yin, Z., Wang, J., & Xu, S. (2015). Modelling the anthropogenic impacts on fluvial flood risks in a coastal mega-city: A scenario-based case study in Shanghai, China. *Landscape and Urban Planning*, 136, 144–155. <https://doi.org/10.1016/j.landurbplan.2014.12.009>
91. Yow, D. M. (2007). Urban Heat Islands: Observations, Impacts, and Adaptation. *Geography Compass*, 1(6), 1227–1251. <https://doi.org/10.1111/j.1749-8198.2007.00063.x>

92. Yu, C., & Hien, W. N. (2006). Thermal benefits of city parks. *Energy and Buildings*, 38(2), 105–120. <https://doi.org/10.1016/j.enbuild.2005.04.003>
93. Zhao, G., Zhao, G., Zhao, G., Zhao, G., Zhao, G., Zhao, G., Pang, B., Pang, B., Xu, Z., Xu, Z., Yue, J., Yue, J., Tu, T., Tu, T., & Tu, T. (2018). Mapping flood susceptibility in mountainous areas on a national scale in China. *Science of The Total Environment*. <https://doi.org/10.1016/j.scitotenv.2017.10.037>
94. Zhao, L., Lee, X., Smith, R. B., & Oleson, K. (2014). Strong contributions of local background climate to urban heat islands. *Nature*, 511(7508), 216–219. <https://doi.org/10.1038/nature13462>
95. Zhu, S., & Mai, X. (2019). A review of using reflective pavement materials as mitigation tactics to counter the effects of urban heat island. In *Advanced Composites and Hybrid Materials* (Vol. 2, Issue 3, pp. 381–388). Springer Science and Business Media B.V. <https://doi.org/10.1007/s42114-019-00104-9>